frontiers | Frontiers in Earth Science

TYPE Original Research
PUBLISHED 20 October 2025
DOI 10.3389/feart.2025.1665965

OPEN ACCESS

EDITED BY
Sanjit Kumar Pal,
IIT(ISM) Dhanbad, India

REVIEWED BY
Claudia Teixeira,
Universidade do Vale do Rio dos Sinos - UNISINOS, Brazil
Mikael Arnemann,
Brava Energia, Brazil

*CORRESPONDENCE
Natasha Stanton,
natasha.stanton@uerj.br

RECEIVED 14 July 2025
ACCEPTED 22 September 2025
PUBLISHED 20 October 2025

CITATION
Stanton N and Gordon AC (2025) New insights into the evolution of hybrid rifted margins: from crustal hyperextension to mantle exhumation at the Santos Basin (Brazil). *Front. Earth Sci.* 13:1665965.
doi: 10.3389/feart.2025.1665965

New insights into the evolution of hybrid rifted margins: from crustal hyperextension to mantle exhumation at the Santos Basin (Brazil)

Natasha Stanton[1]* and Andres C. Gordon[2]

[1]Faculty of Oceanography, State University of Rio de Janeiro, Rio de Janeiro, Brazil, [2]Faculty of Geology, State University of Rio de Janeiro, Rio de Janeiro, Brazil

This study investigates the tectonic, magmatic and sedimentary architecture of the outer Santos Basin, using new ultra-deep high-resolution 3D seismic, gravimetric and magnetic data. We document a major crustal discontinuity that corresponds to a negative magnetic anomaly named Aquarius Lineament (AL). This is associated with N-S striking east-dipping detachment faults - the Aquarius Detachment System (ADS), that extends for more than 270 km. The ADS originated abrupt crustal necking, a core-complex and supradetachment basins. Its location and orientation coincide with major changes in continental lithosphere thickness, Moho depth, and stratigraphy. Seawards from the ADS the ductile lower crust disappears, and there is a transition to a hyperextended domain with deeply incising detachment faults reaching the mantle. The hyperextended domain lies adjacent to a thick magmatic crust that transitions into a domain where the Moho shallows reaching the base of the sediments. Altogether, these contrasting architectural elements reveal a complex lithosphere breakup during the Cretaceous that distinguishes the Santos Basin as a hybrid margin.

KEYWORDS

necking, detachment faults, tectonostratigraphy, hyperextension, mantle exhumation, magmatism, rifting evolution

1 Introduction

Rifted margins have been a subject of extensive research and debate over the last decades due to their geological and economic importance, with great advances in our understanding (e.g., McKenzie, 1978; Wernicke, 1985; Lister et al., 1986; Buck et al., 1988; Brun and Beslier, 1996; Whitmarsh et al., 2001; Pérez-Gussinyé et al., 2001; Leroy et al., 2004; Osmundsen et al., 2002; Lavier and Manatschal, 2006; Autin et al., 2013; Deng et al., 2020; Peron-Pinvidic et al., 2013 and references therein). The search for new hydrocarbon reserves, the continuous technological advancements in deep seismic imaging and drilling have driven exploration towards ultra-deep waters, improving our knowledge about the distal and outer domains.

The evolution of a rifted margin is dependent on the lithospheric responses to local and regional forces, with mechanical, thermal, depositional, and kinematic elements interacting and influencing the final margin architecture (Brune et al., 2023 and references therein). The pre-rift continental lithosphere is heterogeneous, encompassing different terranes with varying tectonic structures. These initial conditions play a fundamental role in the tectonic, magmatic, and sedimentary evolution of rifted margins, in conjunction with strain softening, extension rate and orientation, magmatism, and the interaction between mantle and crust layers (Lavier et al., 1999; Lavier et al., 2000; Tommasi and Vauchez, 2001; Pérez-Gussinyé and Reston, 2001; Naliboff and Buiter, 2015; Duretz et al., 2016; Zwaan et al., 2020). However, the initial conditions are often unrecognized. The thickness of brittle and ductile layers in the considered crustal (Corti et al., 2010; Sutra and Manatschal, 2012) and lithospheric models (Kusznir and Park, 1987; Huismans and Beaumont, 2011; Brune, 2016; Beniest et al., 2018) affects the evolution of deformation and magma budget, resulting in sharp gradients in margin width (Gouiza and Naliboff, 2021; King and Welford, 2022). The continental crust breakup may occur prior or after the mantle lithosphere breakup during depth-dependent extension, implying in "different times of breakup" (Huismans and Beaumont, 2011) that originate various tectonic styles and eventually mantle exhumation (Brun and Beslier, 1996; Whitmarsh et al., 2001; Osmundsen and Peron-Pinvidic, 2018; Deng et al., 2020). Upper and/or lower crust rheological heterogeneities impact the margin segmentation, architecture, and subsidence (Cappelletti et al., 2013; Ros et al., 2017; Stanton et al., 2019). Along with magmatic additions during different stages and within different levels (Decarlis et al., 2018; Nonn et al., 2019; Alvarez et al., 2024), these elements affect the lithosphere response to strain. However, how they interact in space and time leading to final continental lithosphere breakup and seafloor spreading is not completely understood.

The structural evolution of a continental margin plays a fundamental role in the transfer of mantle fluids such as CO_2, H_2, and magma to the crust and sedimentary deposits (Pérez-Gussinyé et al., 2023). Structures control the circulation of hydrothermal fluids, influencing the mobilization, accumulation, and redistribution of hydrocarbons and minerals, favoring or not their formation and/or preservation. Therefore, their recognition is essential for assessing the mineral potential of margins, especially in the transition to a carbon-neutral economy, reducing risks and favoring exploitation.

The Santos Basin is located in the southeastern Brazilian margin (Figure 1) and formed during Early Cretaceous South Atlantic opening (Asmus and Ponte, 1973; Chang et al., 1992; Mohriak, 2003; Araujo et al., 2022). It contributes to approximately 77% of the country's oil production, with potential new discoveries. Despite its importance, the knowledge of the basin's tectono-magmatic evolution is incomplete. The structural framework reveals a complex and multiphase rifting history (Araujo et al., 2022), that resulted in three distinct sub-basins (Figure 1): the Southwest Santos Basin (SWSB), the Central Santos Basin (CSB), and the East Santos Basin (ESB), with differentiated sedimentary architecture, magma budget, and structures (terminology adapted from De Freitas et al., 2022).

The distal Santos Basin structural systems, crustal nature, and tectonic evolution remain mostly unconstrained, as well as its mineral resource potential. Deep crustal structures have been associated with high mantelic CO_2 content in the pre-salt deposits (Ferraz et al., 2019; Plawiak et al., 2024; De Freitas et al., 2022; Juncken et al., 2024), indicating that crustal-scale faults acted as potential pathways for mantle fluids and gases to shallower levels. Similar findings are reported in the South China Sea (Liu et al., 2018), highlighting the importance of the understanding of the deep crustal structures.

Based on new ultradeep high-resolution 3D seismic data (the Viridien Nebula project, Figure 1), gravimetric and magnetic data, we investigate the tectonic, sedimentary, and magmatic evolution of the most distal domain of the Santos Basin. We document the margin transition from 1) crustal hyperextension; 2) to magmatic rifting; 3) to an amagmatic crustal breakup. Based on distinctive potential field, seismic, and sedimentary signatures, we identified a Detachment System and an outer magmatic ridge that reveal an extraordinary outer domain crustal structure and a complex lithospheric breakup evolution.

2 Geological background

2.1 The Santos Basin tectono-stratigraphic and magmatic framework

The onshore continental lithosphere was affected by several convergence-related and extensional events that resulted in the formation of Precambrian sedimentary basins (Heilbron et al., 2000; Schmitt et al., 2016). The Ribeira Belt (RB) consists of several tectonic terranes amalgamated during multiple collisional episodes (from ca. 600 to 510 Ma) in the Brazilian-Pan African orogenic event (Heilbron et al., 2000; Schmitt et al., 2016), with a predominantly NE-SW orientation, comprising anastomosing shear zones, low-angle thrusts, and suture zones (Schmitt et al., 2018; Schmitt et al., 2016; Vieira and Schmitt, 2022). Its easternmost unit, the Cabo Frio Tectonic Domain (CFTD) comprises Paleoproterozoic gneisses interleaved with Neoproterozoic supracrustal nappes of metasedimentary and metabasic rocks (Schmitt et al., 2008; Capistrano et al., 2021; Martins et al., 2021). The CFTD has a NW-SE and N-S structural fabric, relatively oblique to the Ribeira Belt and to the extension direction in the Early Cretaceous rifting.

The Santos Basin at the CSB is a 700 km wide margin, while the conjugate Namibe Basin in the African margin is roughly 150 km wide, constituting one of the most asymmetric segments of the South Atlantic. Gravity inversion, seismology, and seismic refraction studies show a crustal taper from 35 km thick in the Proximal Domain to less than 15 km at the Distal Domain (Figure 1; Evain et al., 2015). The crust and lithosphere are thicker and display lower S-wave velocities in the CSB (Figure 1) than in the ESB (Feng et al., 2007; Evain et al., 2015; Stanton et al., 2019; Haas et al., 2022). These crustal/lithospheric variations significantly impacted the accommodation space and sedimentary evolution of the basin, as indicated by the deepening of the salt base and thicker post-salt successions to the east (De Freitas et al., 2022).

Stanton et al. (2014) proposed the interpretation of the Santos Basin into proximal, necking, and distal domains (following the concepts of Peron-Pinvidic et al., 2013). The Proximal Domain displays NE-SW basement highs and faults that are segmented

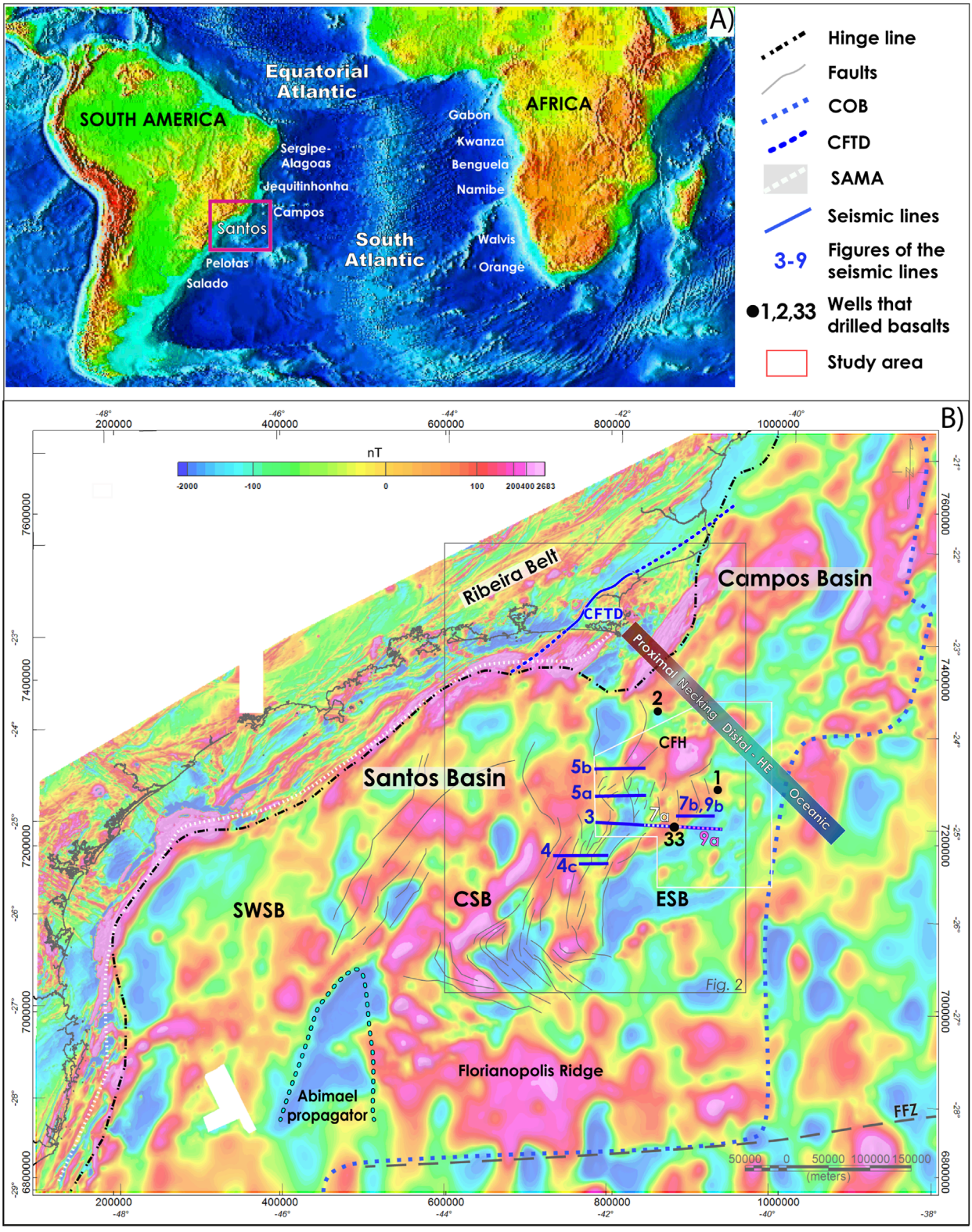

FIGURE 1
(A) Regional bathymetric map of the South Atlantic with the main Brazilian and African basins. **(B)** Magnetic anomaly map reduced to the pole (RTP), with the main tectono-magmatic structures of the Santos Basin and the location of the seismic sections (thick blue lines) in Figures 3, 4, 7, 9 (represented by blue numbers). White and pink dashed lines and respective white and pink numbers refer to the segments of the seismic section in Figure 3 (represented by the number 3 on the map), which are shown in detail in Figure 7A (white number on the map) and 9a (pink number on the map), respectively. Crustal faults from De Freitas et al. (2022); hinge line from Rigoti, (2015); SAMA from Ferreira et al. (2023); margin domains from Stanton et al. (2014), Stanton et al. (2019); Santos COB from Zalán et al. (2011) and this study, and Campos COB from Alvarez et al. (2024); Abimael Propagator from Mohriak (2001); the CFTD (Cabo Frio Tectonic Domain) offshore prolongation at Santos is from Lopes (2023) and at Campos from Stanton et al. (2019) and Strugale et al. (2021). FFZ- Florianópolis Fracture Zone; SWSB- West Santos Basin; CSB- Central Santos Basin; ESB- East Santos Basin; CFH- Cabo Frio High. Black numbers and circles are wells that drilled basalts: 33: 1-Shel-33 RJS and 1: 1-EMEB-1A-RJS, 2: BRSA-905-RJS.

by NW-SE transfer zones, exhibiting short-wavelength magnetic anomalies associated with the offshore prolongation of coastal dyke swarms (Ferreira et al., 2023). The Necking Domain is marked by NW-SE to NE-SW structural highs and faults (Stanton et al., 2014; De Freitas et al., 2022) and an almost continuous, positive magnetic lineament known as SAMA (Ferreira et al., 2023; Figure 1) related to an intruded and faulted crust. The Distal Domain is distinguished by a hyperextended crust with upper continental crustal blocks, deep and long-offset detachment faults and possible extensional allochthons, accompanied by intense volcanism (Araujo et al., 2022; Arnemann et al., 2023), and by a region of varying crustal thickness and debated nature.

The basement framework displays a regional strike rotation of the structural trends from southwest to northeast, from NNE-SSW to NW-SE in the SWSB, transitioning to an S-shape fault's trend in the CSB, and to NNE-SSW structural trends at the ESB (Araujo et al., 2022; De Freitas et al., 2022). Although the most distal part of the basin remains poorly characterized, it exhibits important magnetic and gravity anomalies associated with magmatic structures such as the Tupinamba High (Gomes et al., 2009; Karner et al., 2021; De Freitas et al., 2022), the volcanic ridge bordering the Abimael propagator (Mohriak, 2001; Candeias et al., 2024) the hyper-extended stage volcanism at the southern Santos Basin (Arnemann et al., 2023), and the Florianopolis Ridge within an area proposed as a "resistant block" (Zalán et al., 2011). The Florianopolis Ridge controlled the formation of the giant Aptian salt basin and influenced its oil resources (Szatmari and Milani, 2016).

Different interpretations are proposed for the nature of the basement of the Santos Basin, such as thinned continental crust transitioning to intruded continental crust oceanward (e.g., Karner, 2000; Mohriak et al., 2002; Moulin et al., 2013; Kumar et al., 2013; Evain et al., 2015), hyper-extended and magma-rich (Karner et al., 2021; Arnemann et al., 2023), or serpentinized mantle exhumed at the distal margin (Zalán et al., 2011). Recently, Pérez-Gussinyé et al. (2023) proposed an intermediate margin type for the Santos Basin, characterized by significant magmatism during crustal thinning, along with detachment faults, but without SDRs or exhumed mantle. These contrasting interpretations are due to the great complexity of the geophysical signatures within the basin and the lack of basement drilling. It has only been sampled by the well 1-BRSA-905-RJS at the Cabo Frio High (CFH, Figure 1), where the crystalline crust of the CFTD is present, dated at 1.96–1.98 Ga (Carmo et al., 2017).

The Santos Basin evolution encompassed four major tectono-stratigraphic phases: rift-onset flood basalts followed by syn-rift, post-rift, and drift supersequences (Chang et al., 1992). The basin stratigraphy includes a syn-rift supersequence comprising continental siliciclastic sediments, lacustrine carbonates, and shale deposits accumulated between approximately 130 and 122 Ma, and corresponds to the Piçarras and Itapema formations (Moreira et al., 2007; Alkmim et al., 2025). During this tectono-stratigraphic stage, both the source rock and the lower pre-salt carbonate reservoir of the giant pre-salt oil fields were formed. The post-rift supersequence includes proximal siliciclastic deposits, thick lacustrine carbonates (upper pre-salt reservoirs), and an extensive evaporite layer capping the succession. It is bounded at the base by a rift-related unconformity dated to around 122 Ma and overlain by thick evaporites deposited between approximately 120 and 118 Ma (Alkmim et al., 2025), followed by continental breakup at ~118 Ma (Alkmim et al., 2025).

Later, the basin evolved into a marine divergent setting in the Late Aptian, with the initial development of an extensive carbonate platform and marls (Spadini et al., 1988), followed by open marine depositional systems since the Cenomanian (Mohriak, 2003; Moreira et al., 2007). Six major magmatic episodes are reported throughout the rift-onset, syn-rift, post-rift, and drift stages (Moreira et al., 2007; Gordon et al., 2023a), with varying geochemical affinities and emplacement mechanisms within the proximal and distal margins (Carvas et al., 2021; Gordon et al., 2023a).

3 Database and methods

The present contribution is based on borehole, reflection seismic, gravity and magnetic data analysis. The seismic sections at Figure 4 are depth-converted 3D lines from the "Agência Nacional do Petróleo" (ANP) public database; the sections at Figures 3, 5, 7, 9 (locations in Figure 1) are courtesy of Viridien Company and correspond to the "Nebula C project" (Figure 1B), a 3D seismic survey recently acquired with remarkable deep crustal imaging down to 20 km depth that illustrates the crustal and upper mantle architecture, partially published by Juncken et al. (2024). Seismic velocities displayed in Figure 6C were obtained from PSDM interval velocities from a Full Wave Inversion model (FWI, Huang et al., 2021). The seismic velocity model used comprised FWI velocities from the seafloor down to top salt. The salt layer was modeled using salt flooding velocities. From the salt base down to 20 km the model used tomographic velocities. Well data corresponds to ANP public wells 1-Shel-33-RJS and 1-EMEB-1A-RJS (Figure 8).

The magnetic grid (Figure 1B) is from Stanton et al. (2019) and Ferreira et al. (2023). The original data is a compilation of ten onshore and offshore aeromagnetic surveys, one marine survey, and satellite data to fill the most distal parts of the margin (for survey acquisition details, see Ferreira et al., 2023). The onshore data was provided by the Geological Survey of Brazil (CPRM), the "Companhia de Desenvolvimento Econômico de Minas Gerais" (CODEMIG). The offshore data was provided by the ANP, and the satellite data is from EMAG2 V3 (Meyer et al., 2017). Each survey was processed separately due to the different acquisition parameters (line spacing, flight height, and orientation). We removed the Regional Magnetic Field by subtracting the IGRF model and applied microleveling to the data (Minty and Luyendyk, 1997). The magnetic anomaly grid has ×250 250 m of data interpolation. It was Reduced to the Pole (RTP; Baranov, 1957; Baranov and Naudy, 1964) using the mean values of inclination and declination from the paleomagnetic data from Raposo et al. (1998) in order to place the anomalies over their respective sources.

The gravity and magnetic 2D forward modeling are based on the method of Talwani (1965). The physical properties (density, magnetic susceptibility, and remanence) of the layers used in the models consist of: susceptibility values obtained from diabases mapped onshore (unpublished), from basaltic rocks sampled at the Santos Basin, and general values in the literature (Carmichael, 1982) (Table 1). We applied susceptibility and remnant magnetization parameters for the igneous rocks since the magnetic

TABLE 1 Physical parameters for the 2D forward modeling.

Lithologies/Properties	D (kg/m3)	K (SI)	NRM (A/m)
Sediments	2000–2,500	0.0001	0
Sediments and volcanics	2,500–2,700	0.08–0.09	4
Upper crust	2,670	0.001	0
Lower crust	2,900	0	0
Magmatic (intruded) crust	2,800–2,900	0.05–0.09	4
sills	2,700	0.05–0.09	4
gabbros	2,850–2,900	0.05	4
underplating	3,000	0.02	1
Serpentinized mantle	2,600–2,800	0.02–0.06	4
Mantle	3,330	0	0

anomalies result from the sum of both remnant and induced magnetizations. The magnetic contribution of sedimentary and most continental basement rocks is usually minimal or negligible.

4 Observations

4.1 The Aquarius Detachment System (ADS)

We characterized a crustal-scale fault system at the ESB referred hereafter as the Aquarius Detachment System (ADS). This structural system is associated with an abrupt lateral change in the magnetic anomalies, coinciding with a negative zone trending N-S here named the Aquarius Lineament (AL; Figure 2). Across the AL, seismic data reveals contrasting faulting styles and basement seismic facies indicating a lateral heterogeneity within the crust (Figure 3 Zones I and II; Table 2 in supplementary files).

A set of synthetic listric, east-dipping faults with moderate displacement are observed, with a first large-scale detachment (the Breakaway Fault BA1, Figure 4) beginning at 40–50 km to the west of the ADS. These faults sole out at a level approximately located at 10 km depth, on the top of a strongly reflective lower crust, thus interpreted as the crustal brittle-ductile transition, where the master detachments root. They form depocenters that accommodate thick sedimentary wedges (Figure 3 Zone II, and detail in Figure 4). Along the ADS the upper crust is characterized by: 1) continuous subparallel east-dipping reflectors in the upper unit, interpreted as rift-onset flood basalts (similar to those drilled at the adjacent Tupi High, Gomes et al., 2009), and 2) a reflection-free lower unit (Figure 3). The lower crust is reflective with parallel-subparallel west-dipping reflectors bottomed by the Moho (at c.a. 20–22 km depth) and topped by a continuous low acoustic impedance reflector (Figure 3 Zone I; Table 2).

The ADS displays a Master detachment (Breakaway Fault, BA2 in Figure 4) exhibiting large magnitude displacements and listric geometry that affects various crustal levels. It extends continuously for at least 270 km, striking N-S with subtle NNE-SSW inflections in map view (Figure 2). The ADS also comprises several synthetic faults that reach the Moho, forming "breakaway blocks" (Masini et al., 2011; Figure 3 Zone II, and 7), with listric to flat-ramp fault geometry, locally convex-upward. Eastwards of the master detachment (ADS in Figure 3 Zone II, and BA2 in Figure 4) there is a lateral change in detachment rooting level and geometry, accompanied by the progressive disappearance of the reflective lower crust as the entire crust thins. The master detachment exhibits secondary faults that merge into the BA2 forming incising fault splays (Figure 4C).

The lower crust exhibits semi-continuous bright reflectors that rise to the east and are warped beneath the ADS (Figure 3, at the boundary between Zones I and II) probably representing shear zones. Along the ADS both Moho and deeper reflectors in the upper mantle are flexed upward, reaching 11–12 km in depth beneath wide half-grabens and culminating in a major crustal necking.

As the detachment faults reached deeper levels down to the Moho along the ADS, they promoted large-scale horizontal displacement, creating over-tilted and rider blocks. The ADS faults either sole out along the crust-mantle boundary or cut the Moho. Locally, the top basement reaches the base of the salt as evidence that the footwall was isostatically uplifted and back rotated as the hanging wall progressively moved away by the detachment, giving rise to the formation of supradetachment basins (Figures 4, 5). These basins accommodate 2–6 km thick sedimentary wedges, deposited in multiple syn-tectonic packages (represented by different colored sequences in Figures 4B,C), with reflectors truncated by the regional Syn-rift Unconformity (~123 Ma, Gordon et al., 2023b; Alkmim et al., 2025).

The detachment faults change their geometry to the east, becoming bowed up at the zone of maximum crustal necking along the ADS (Figure 3, Zone II; Figure 5). This probably resulted in the detachments becoming unfit to accommodate displacement, which was then transferred eastwards, generating progressively younger

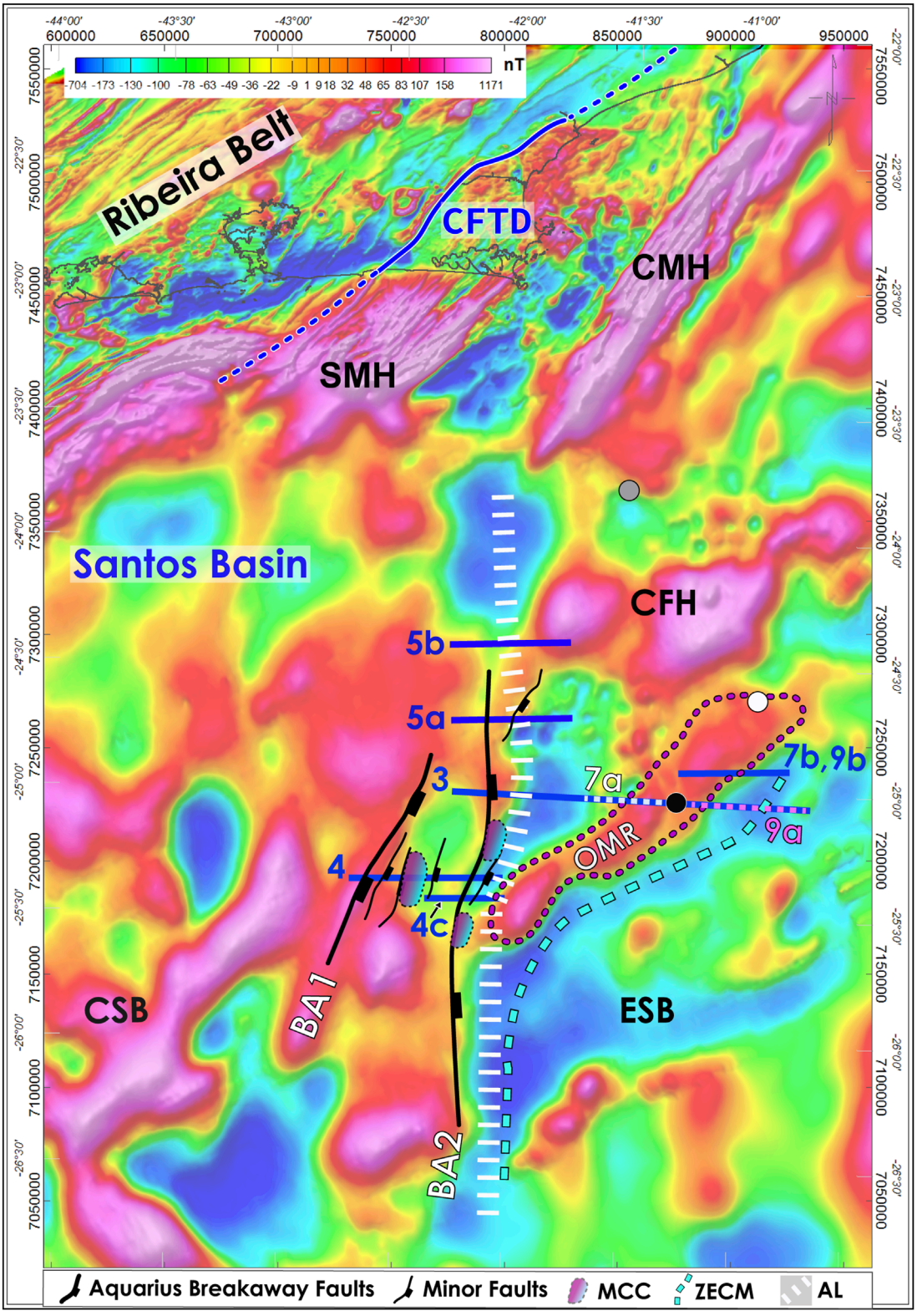

FIGURE 2
Magnetic anomaly map reduced to the pole of the study area representing the location of the seismic sections displayed in Figures 3, 4 (blue lines), 7 (dashed white line) and 9 (dashed pink line); the Aquarius Lineament (AL), the main detachment faults and the interpreted tectono-magmatic features. SMH- Santos Magnetic High; CMH- Campos Magnetic High; CSB- Central Santos Basin; ESB- East Santos Basin; CFH- Cabo Frio High, BA1 and BA2 - breakaway faults of the Aquarius Detachment System (ADS); OMR- Outer Magmatic Ridge; ZECM- Zone of exhumed continental mantle. Circles are wells that drilled basalts: black: 1-Shel-33-RJS, white: 1-EMEB-1A-RJS, grey: BRSA-905-RJS.

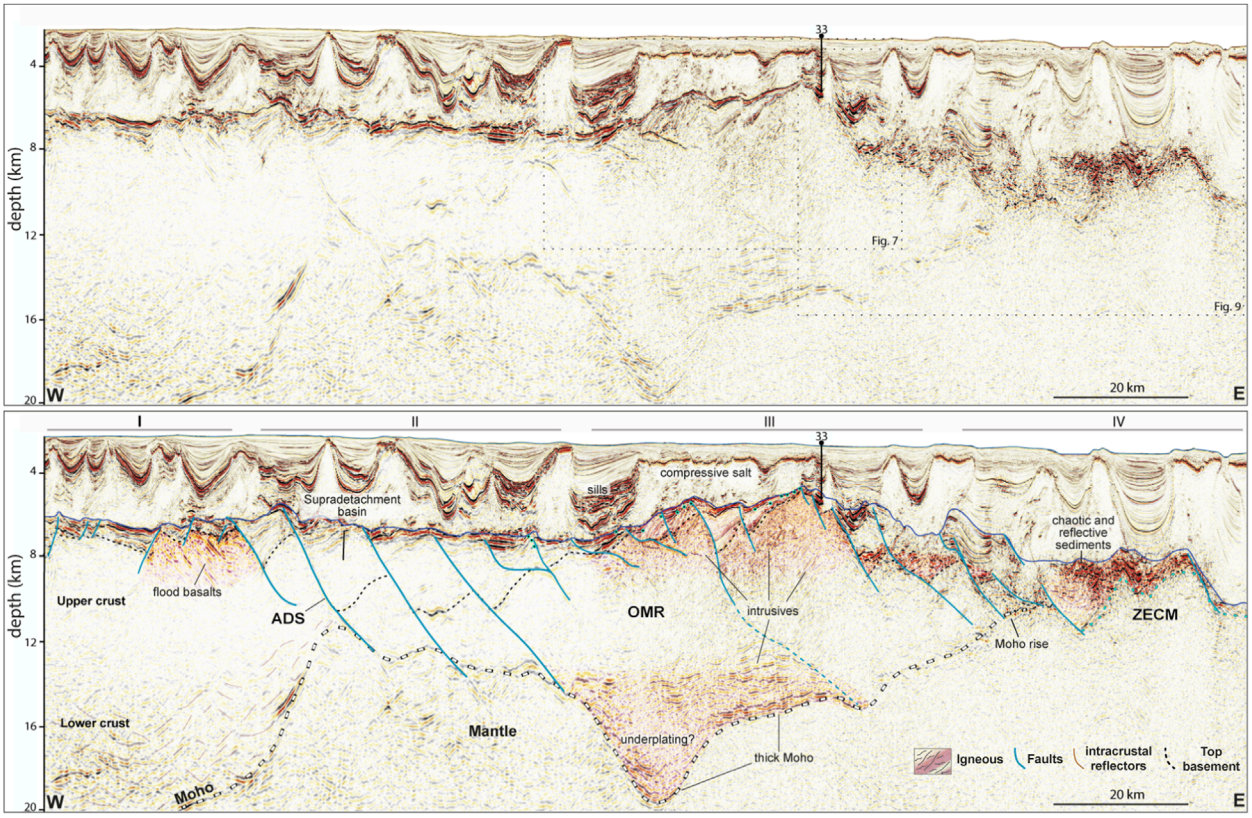

FIGURE 3
Upper section: Deep seismic section showing the crustal and sedimentary architectures of the distal and outer Santos Basin. Lower section: Interpreted seismic section. ADS- Aquarius Detachment System; OMR- Outer magmatic ridge; ZECM- Zone of exhumed continental mantle; I to IV- Zones of distinct geological and geophysical characteristics (see text for discussion); 33- well 1-Shel-33-RJS that drilled basalts. Small black-cyan circles indicate the toplap geometries/erosional unconformities. Location in Figure 1.

faults and basins (Figures 4B, 5). The convergence of deep crustal reflectors beneath the ADS at the zone of maximum crustal necking suggests that deformation was achieved by coupling between upper crustal faulting and lower crust shear zones, which resulted in a hyperextended crustal domain. This domain, at the most distal part of the basin, is spatially disconnected from the oceanic domain by a region of thickened crust, described in the next section.

4.2 The outer magmatic ridge (OMR)

The magnetic map (Figures 1, 2) displays nearly continuous and elongated high-amplitude positive magnetic anomalies (>400 nT), trending NE-SW for 220 km along the ESB. It has width and length of approximately 30–40 km and 100 km, respectively. The seismic data and potential field modeling (Figures 3, 6, respectively) show a large basement high associated with a region of deeper Moho that corresponds to a ridge-shaped magnetic high. The crustal thickness varies from 4 to 5 km to the west (at the ADS) to 12–14 km at the basement high. The crust exhibits lateral and vertical seismic facies variation, transitioning from a highly reflective lower crust to a low-reflective middle crust and to an upper crust exhibiting parallel and tilted reflectors, possibly representing flood basalts.

The potential field modeling indicates a vertical gradient of densities varying from 2,800 kg/m3 at the upper part of the basement (see purple blocks in Figure 6), which could represent basic igneous intrusives and/or the flood basalts that overlain the top basement within the Santos Basin (Moreira et al., 2007). Below these blocks, the upper crust with densities of 2,670 kg/m^3 could represent metamorphic rocks. A slight increase in density at the middle crust to 2,700 kg/m3 may correspond to the presence of denser metamorphic rocks. The higher densities obtained for the lower crust (2,900 kg/m3) and its root (3,000 kg/m3) can represent ultrabasic igneous rocks or amphibolites. The seismic velocity model (FWI) indicates an upper crust with a gradient of velocities from 5,800 m/s to 6,800 m/s, showing a slight increase associated with the purple blocks, and a lower crust with a velocity higher than 7,000 m/s along the OMR (Figure 6). The wells drilled on the presalt section over the OMR range between 2,500 and 2,800 kg/m3 for the basalts intercalated with the sedimentary deposits, displaying compatible densities with those obtained from the 2D modeling (Figure 8).

The basement within the OMR exhibits subparallel reflectors of variable amplitude, likely indicating extensive igneous intrusions. Over the structural high, the syn-rift deposits are distinguished by tilted high-amplitude reflectors, which most likely represent intercalations of sedimentary and igneous, as observed in wells

TABLE 2 Summary of the geophysical and geological characteristics of a hybrid rifted margin from the example of the Santos Basin.

	The hybrid margin type			
	Aquarius Detachment Sytem(ADS)		Outer Magmatic Ridge (OMR)	Outer Domain
Sub-basin	CSB	ESB	ESB	ESB
Zones	I	II	III	IV
Shape & structural orientation	Linear features trending NE-SW with subtle NNE-SSW inflections	Linear features trending N-S, extends from 26°S to 24°S for at least 270 km.	Elongated body of ~ 220 km ridge-shaped NE-SW oriented, 24°30' to 25°45' S	About 120 km swath before reaching oceanic crust
Upper Crust	1) Continuous subparallel east-dipping reflectors in the upper unit, interpreted as rift-onset flood basalts, and 2) a reflection-free lower unit		Low reflected upper crust topped by parallel and tilted reflectors	Semi-transparent basement seismic facies without Moho reflector - possible domain of mantle exhumation
Lower Crust	Higlhy reflective; subparallel west-dipping reflectors bottomed by the Moho and overlained by continuous low acoustic impedance reflector indicating lower velocity at the lower crust, which decreases in thicknes (c.a. 3 km thick) towards the ADS, and disappears eastward.	Semi continuous bright reflectors, that are shallow to the east and are warped beneath the Master detachment (BA2) likely representing shear zones.	Highly reflected crust, exhibiting locally a Moho deepening (root) suggesting underplate intrusions	
Moho Depth	20 to 22 km	11 to 12 km, formation of a major crustal necking	~20 km	~10 km
Fault styles	A set of synthetic listric east-dipping faults, moderate displacement. First large-scale detachment (Breakaway Fault 1, BA1) beginning c.a. 40-50 km to the west of the ADS. They root at approximately 10 km depth (Conrad dicontinuity).	1) a Master detachment (BA 2), with large magnitude displacements, moderate dips and listric geometry that affects various crustal levels, 2) large-magnitude faults reaching the Moho, forming "breakaway blocks", listric to flat-ramp fault geometry, locally convex-upward.	Tectonically rotated normal faults	Series of large litric faults reaching Moho.
Magnetics	Large positive anomalies trending ENE-WSW, up to 300 nT	Wide area of negative magnetic anomalies	High amplitude (400 nT) and ridge-shaped magnetic anomalies	A negative magnetic anomalies, with isolated sub-rounded and low amplitude positive anomalies
Rift Section	Large wedge depocenters, up to 2300 m thick deposited in two synrift packages: upper and lower (thicker)	Wide half-grabens, with supradetachment basin developed	Up to 3500 m thick, display rotated, inverted and folded half-grabens	The presalt is reflective and Higly intruded, less than < 3 km thick
Basement Tectonics	Thick crust, preservation of upper and lower crust	Hyperextended and necking zone	Evidence of tectonic reactivations, including: 1) inversion of syn-rift half-grabens; 2) creation of a compressional (pop-up) block of basement; 3) faults affecting up to the salt base	Mantle exhumation and higly intruded pre-salt sequences
Salt Tectonics	Large salt dome and walls, base of salt from ~5400 to 6600 m depth.	Large salt dome and walls, base of salt from ~ 6600 to 6600m to 7400m depth.	Compressive salt structures, indicate reactivation resulting in a elevated topography that acted as a barrier for the salt flowing. Salt base at 4800 m depth.	Isolated salt domes, deeper salt base (~8200 to 10300 m).

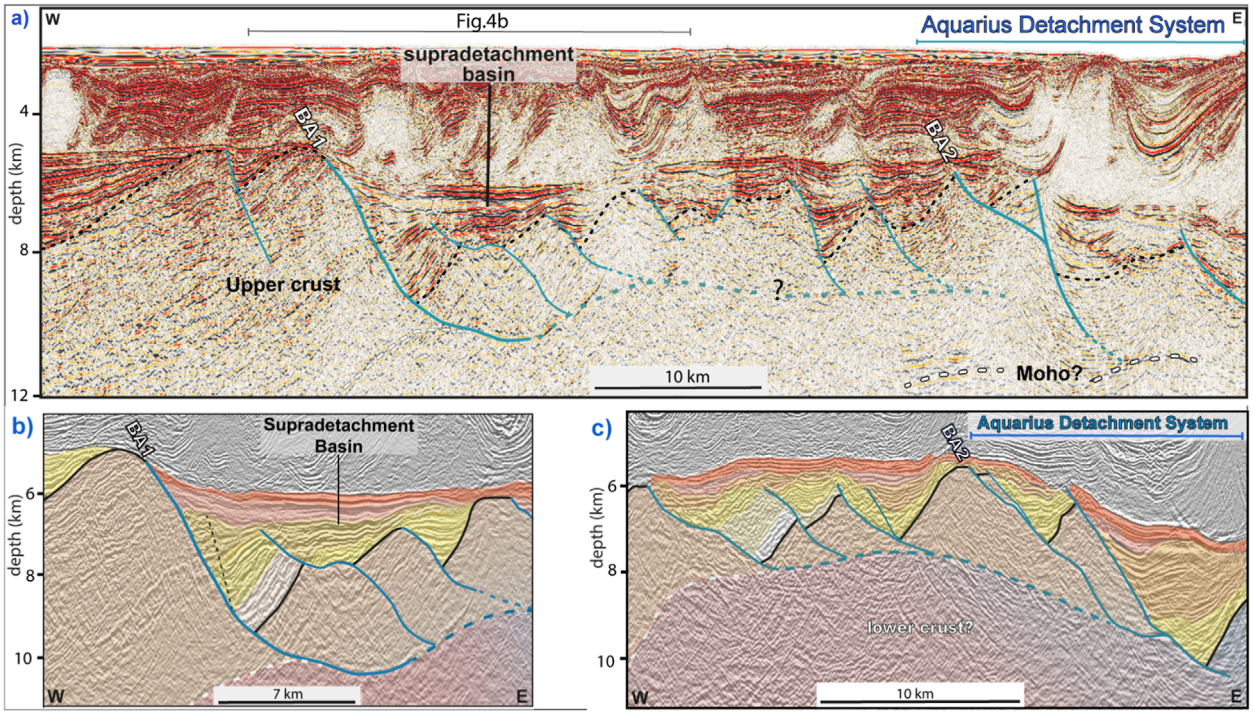

FIGURE 4
(a) Seismic sections illustrating the Breakaway faults BA1 and BA2 (ADS) and the multiple syn-tectonic units, represented by yellow to orange colors in: **(b)** detail of the BA1 and the supradetachment basin; and **(c)** detail of BA2 (ADS) and the change in the tectonostratigraphy eastwards. The blue dashed lines represent the possible prolongation of the faults within the crust. For location see Figure 1.

Shell 33 and EMEB 1a (Figure 8). The OMR exhibits evidence of tectonic reactivation, including 1) inversion of syn-rift half-grabens; 2) formation of compressional (pop-up) basement blocks; and 3) faulting that extends up to the base of the salt layer (Figures 3, 7). Additionally, the presence of compressive salt structures overlaying the OMR suggests tectonic reactivation generating significant topographic relief, which probably acted as a barrier for the salt flowing oceanwards. Based on the unconformity at the base of the salt dated at ~ 120 Ma (Alkmim et al., 2025) and the volcanic rocks intercalated with syn-rift deposits (Shel 33 well, Figures 1, 3) and the pre-salt carbonates (EMEB 1a well; Figure 8), this may correspond to the age of the OMR emplacement and will be discussed in section 5.2.

The study area shows evidence of recurrent magmatic activity, like saucer-shaped, high-amplitude reflectors observed in the post-salt sequence above the OMR, which are indicative of igneous intrusions during the drift stage.

Based on its shape, seismic characteristics, crustal thickness, and high-amplitude positive magnetic signature, we interpret the outer high as a magmatic ridge. Since it constitutes a distal structure at the Santos Basin, we named it Outer Magmatic Ridge (OMR). The deformed syn-rift strata, downlap geometry and top truncation phenomenon, as well as the strong intracrustal reflections indicating intrusives within the outer high, allow us to infer that the original basement had been reworked by magmatic activities, resulting in inversion of the overlying syn-rift strata due to the upward push from the magmatic intrusions and the isostatic compensation. Its root (where Moho reaches the greatest depths) exhibits strong subparallel reflectors, densities of ~3,000 kg/m3 and velocities higher than 7,000 m/s (Figure 6A), which correspond to intermediate density and velocity values between normal continental crust and lithospheric mantle. The Moho reflector on the sides and below the OMR is characterized by arrays of high-reflective bands of layered reflectors ~2–3 km thick, that are interpreted to represent mantle-derived mafic sills, indicating significant magmatic underplating.

The potential field modeling best fit within the OMR indicates the massive presence of basic igneous rocks at various levels within the entire crust (Figure 6). The model that considers a slightly intruded continental crust does not adjust with the observed magnetic anomalies, since these require a large amount of rocks with very high magnetization. In general, continental crustal rocks are characterized by low susceptibilities and remanence values, with few exceptions. In the study area, the susceptibility values measured at the continental rocks of CFTD show values in the range of 0.0001–0.007 with a mean of c.a. 0.001 SI (Lopes, 2023), while the mafic igneous rocks exhibit mean values of 0.05, reaching 0.09 SI. It is important to highlight that the proposed nature for the basement, based solely on geophysical data, remains a significant challenge, especially in the distal domain and due to the non-uniqueness aspect of geophysical methods. This domain may contain crystalline crust and/or serpentinized mantle, with or without magmatic additions in varying amounts. Based on such uncertainties, we explored through the 2D potential field model and the velocity gradient the best fit for the composition of the crust at the study area,

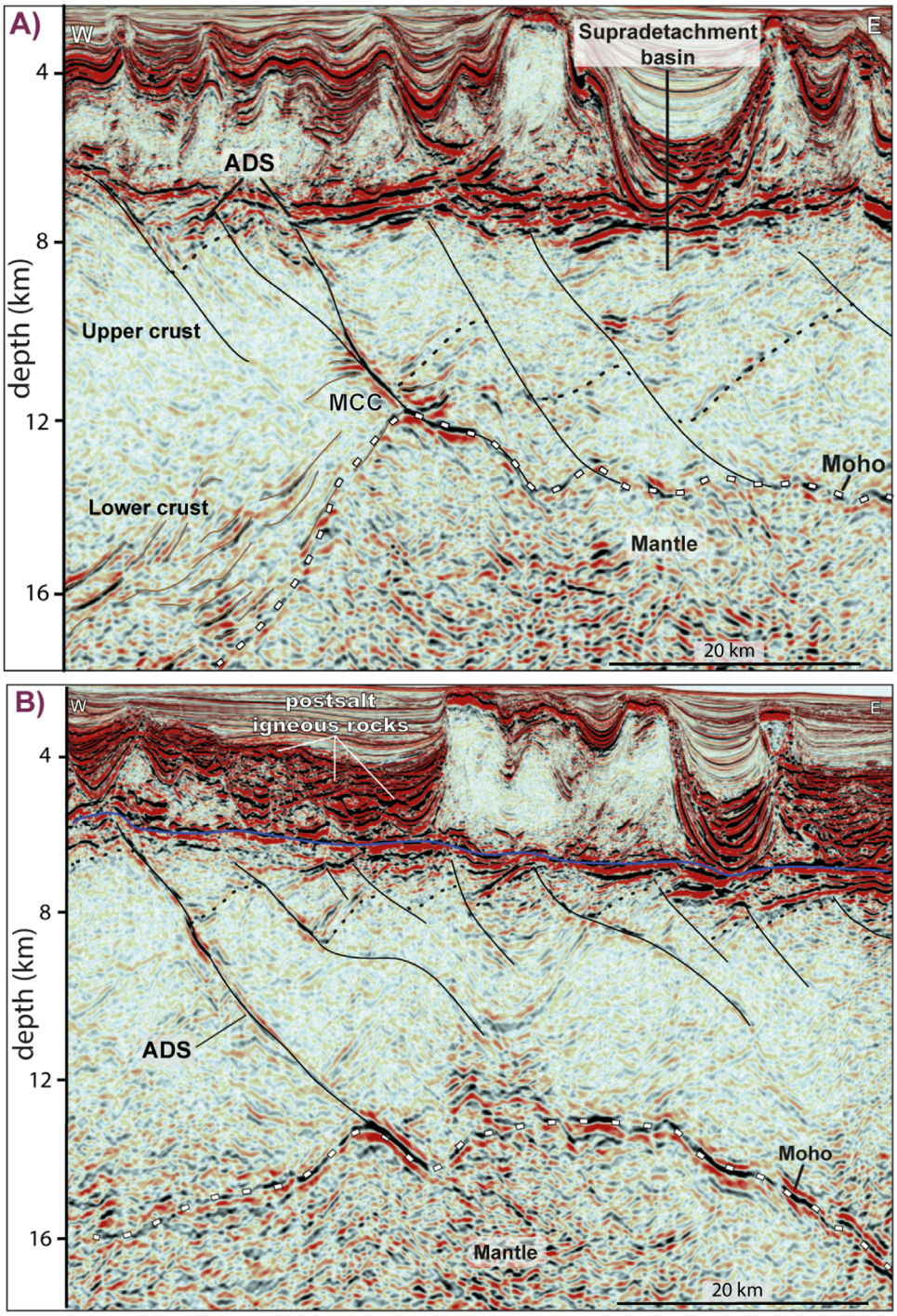

FIGURE 5
Detail of 3D seismic sections (see location in Figure 1) showing the geometry of the crustal necking and faults along the Aquarius Detachment System (ADS). Note the abrupt lateral variation in crustal thickness with progressively deeper incising detachment faults that reach the Moho, and the exhumation of lower crust forming a metamorphic core-complex (MCC) at **(A)**. At **(B)** the reflective lower crust is observed across the section and most of the detachments root at shallower crustal levels (10–11 km).

applying different basement lithologies (displayed in Figures 6B,C), based on the joint combination of geophysical signatures, which are summarized in Table 2.

Therefore, the basement nature within the OMR probably corresponds to a highly altered crust. The structural inversion and deformed strata on the top of the OMR imply that the original crust was faulted and had sedimentary filled half grabens prior to its formation, probably corresponding to a hyperextended crust similar to that observed continentward. The stratigraphic evidence from the exploratory wells 1-Shel-33-RJS and 1-EMEB-1A-RJS that drilled

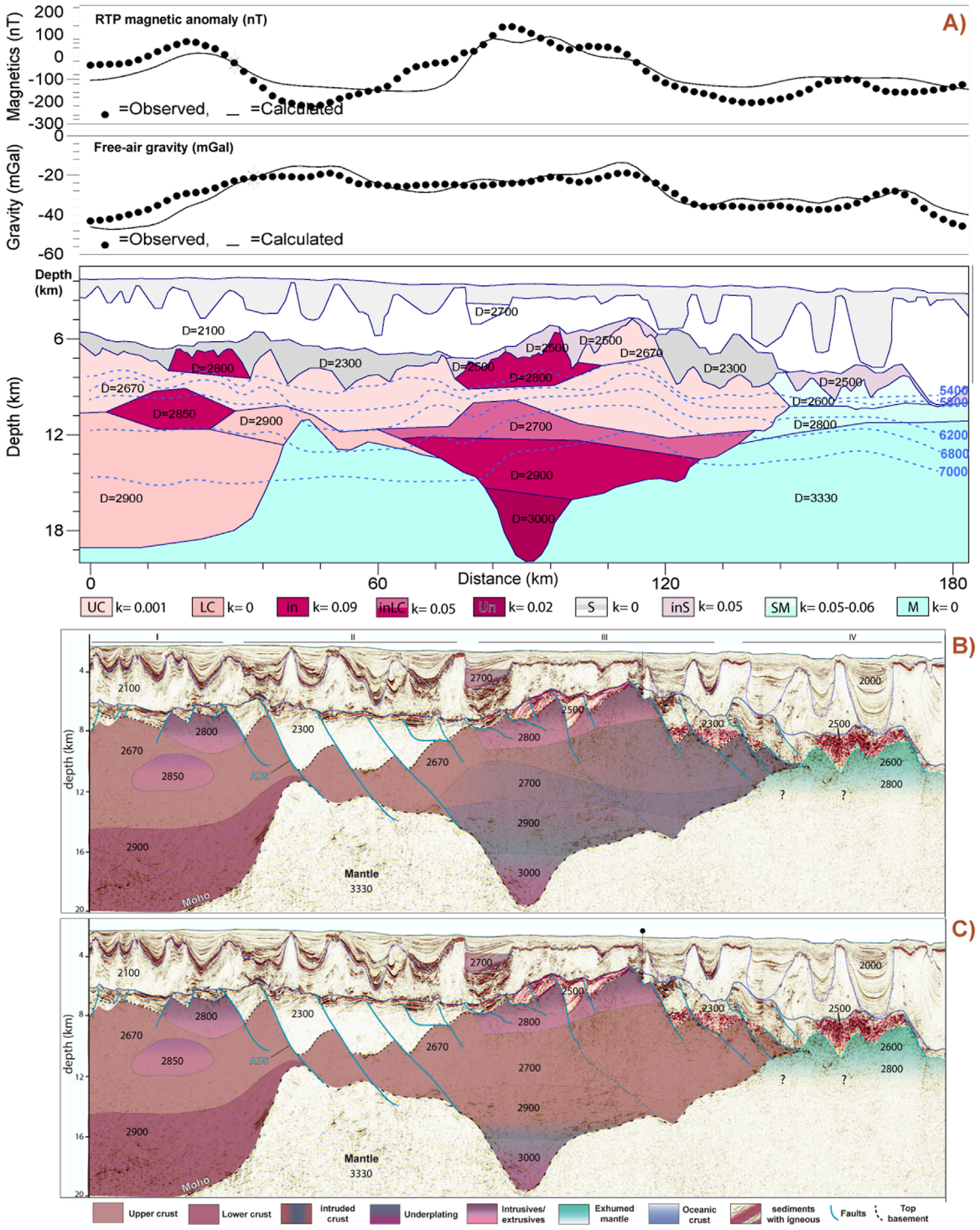

FIGURE 6
(A) 2D forward gravity and magnetic modeling of the seismic section of Figure 3, displaying the basement physical characteristics. We propose 2 different scenarios for the nature of the basement at the distal and outer Santos Basin: **(B)** SCENARIO 1- a transition from a thick continental crust (Zone I), to a hyperextended continental crust (Zone II), to a highly intruded crust (Zone III), and to mantle exhumation (Zone IV); **(C)** SCENARIO 2- a transition from thick continental crust (Zone I) to a hyperextended continental crust (Zone II), to a thick continental crust with less intrusions (Zone III), and to mantle exhumation (Zone IV). Black numbers within the blcoks are densities from the 2D model in kg/m3; blue dashed lines and blue numbers refer to seismic velocities in km/s from the FWI model. The purple blocks overlying the upper crust represent the proposed basalt floods of the Camboriu Fm. Which cover the top basement at the Santos Basin (Moreira et al., 2007) and possible related crustal intrusives. The legend for the modeled blocks at the bottom of **(A)** display the susceptibility values (k) in SI: UC- upper crust; LC- lower crust; in-igneous intrusives; inLC- intruded lower crust; UN- underplating; S- sediments; inS- intrusives and sediments; SM-serpentinized mantle; M-mantle. The remanent magnetization values for each layer are provided in Table 1. A model for scenario 2 displaying unfitting magnetic curves is included as supplementary materials.

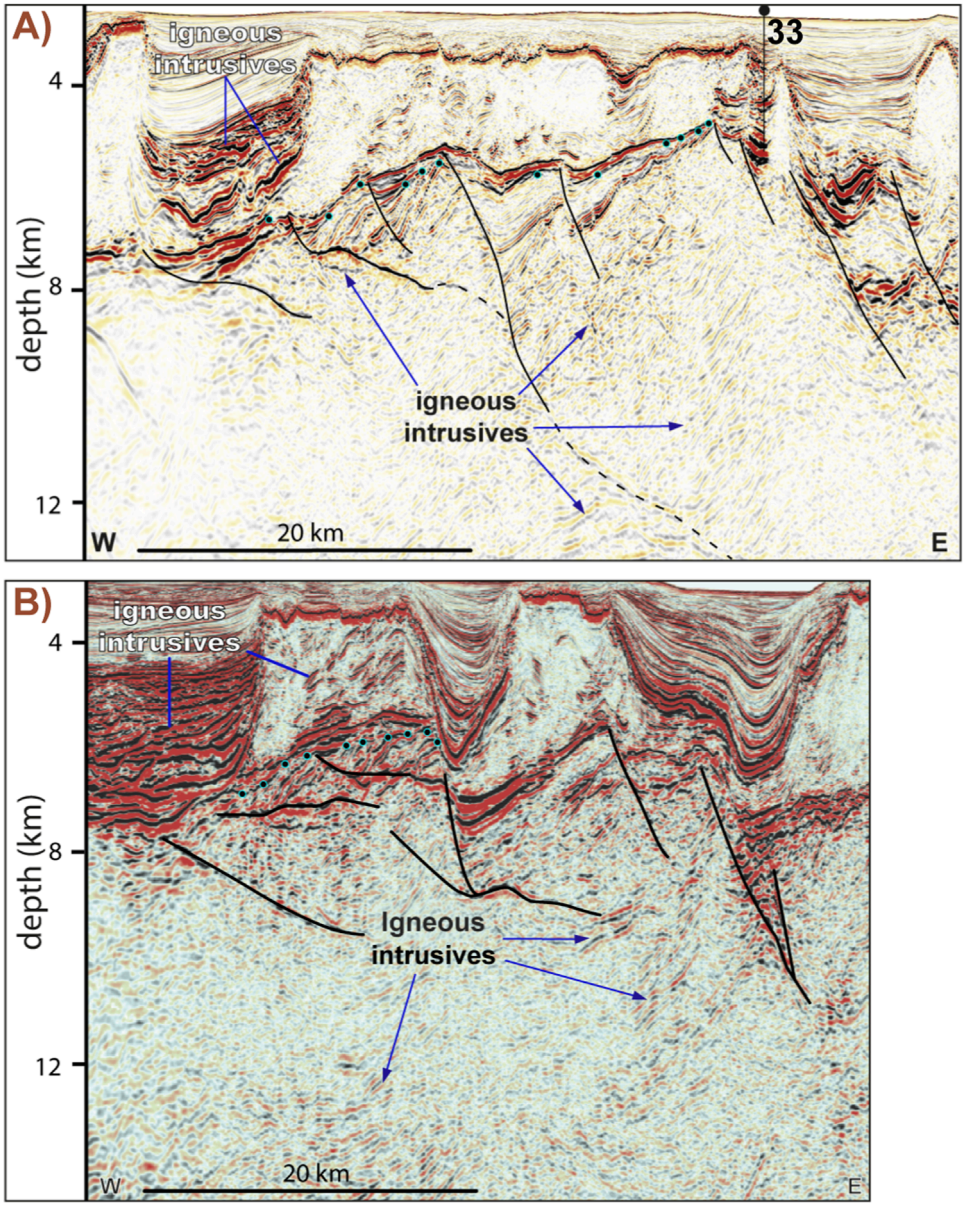

FIGURE 7
Details of 3D seismic lines displaying the Outer Magmatic Ridge (see location in Figures 2, 3). Note the uplift of the pre salt strata, the structural inversion of the half-grabens and overlying compressional salt structures. High-energy intracrustal reflectors indicate the presence of intrusive rocks. Black circle refers to well 1- Shel-33-RJS that drilled basalts **(A)**. Note post-salt sills in **(B)**. Small black-cyan circles indicate the toplap geometries/erosional unconformities.

the OMR indicate that the half-grabens were filled with typical pre-salt deposits (Figure 8 and location in Figures 1, 2). Well 1-Shel-33-RJS (33 in Figure 1) drilled approximately 1,300 m of salt (mainly halite and anhydrite), a thin post-rift section of marls (c.a. 36 m), an upper rift section of 154 m of calcilutite, and a lower rift section, 460 m thick, of volcanic rocks with several siltstone intercalations. Well 1-EMEB-1A-RJS, located 45 km northeast of the seismic example in Figure 3, penetrated 1860 m of salt (mostly halite, with anhydrite and some carnallite) and a 580-m-thick pre-salt section. The pre-salt section consists of an upper layer of 190 m of carbonate rocks and a 390-m lower layer of volcaniclastic rocks (summing up to 80% of the section) and carbonate intercalations. Both wells exhibit pre-salt carbonate rocks (predominantly deposited in low-energy environments, most likely in distal lake settings) and CO_2 contaminants. In view of the present evidences, we propose two distinct scenarios to illustrate the nature of the basement of the OMR: 1- composed by a continental crust highly intruded (>80%) by igneous rocks (Figure 6B) or 2- by a continental crust only slightly intruded by igneous rocks (Figure 6C). The scenario 2 is difficult to reconcile with the observed crustal root under the OMR and the potential field signature, therefore we favor the scenario 1.

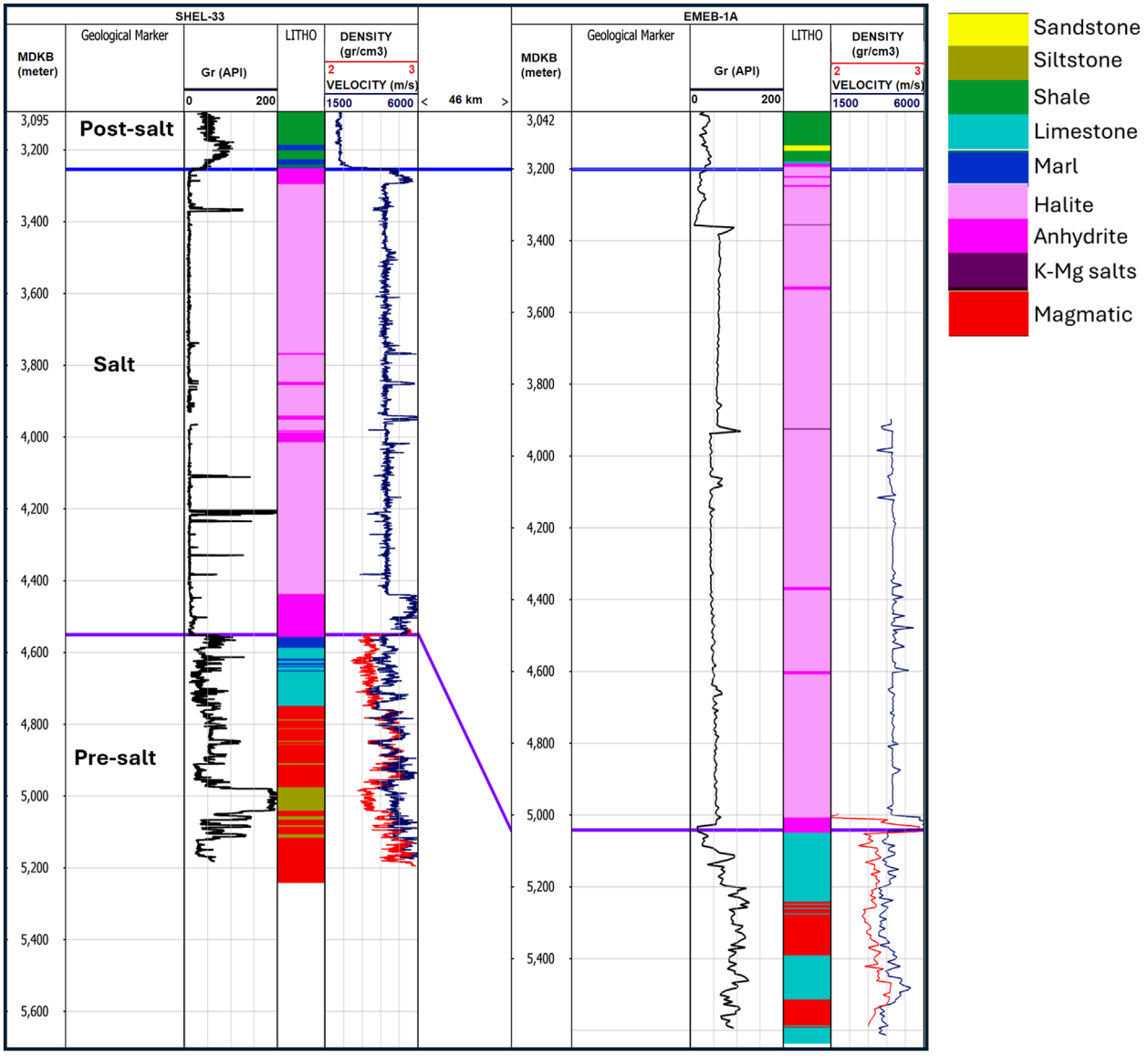

FIGURE 8
Well log data from wells 1- Shel-33-RJS e 1-EMEB-1a-RJS that drilled basalts at the OMR. Location in Figure 1. The stratigraphy in these wells presents, at the base, Barremian to Aptian syn-rift shales and siltstones from the Itapema Fm., recently U/Pb dated in 126–122 Ma (Alkmim et al., 2025); Aptian lacustrine carbonates from the Barra Velha Fm (c.a.122-119 Ma); Aptian evaporites from the Ariri Fm. (c.a. 120–118 Ma); and at the top occur Albian shales and carbonates.

4.3 The outer domain of the east Santos Basin

At the most distal part of the ESB (Zone IV in Figure 3 and detail in Figure 9) a steady rise of the Moho reflector seems to reach the base of the pre-salt strata. The latter is constituted by highly reflective layers that overlie a reflection-free basement associated with low-amplitude, negative magnetic anomalies (Figure 2). The potential field modeling indicates low densities for the upper basement in this region, increasing gradually with depth from 2,600 to 2,800 kg/m^3. Such density variation is in accordance with those observed at the zone of subcontinental serpentinized mantle of the Iberian margin. The serpentinization process results in the decrease of the peridotite densities from 3,330 to as low as 2,500 kg/m^3 (Miller and Christensen, 1999; Dean et al., 2000). The FWI velocity model indicates a range of compressive-wave velocities (from 5,800 to 6,200 m/s). The vertical gradients of density and velocity are sharp and may indicate various lithologies with variable silica content, from acid to intermediate rocks; nevertheless, they do not correspond to expected values for typical mantle rocks. In conjunction with the rise of the seismic Moho to the base of the sediments and the low-amplitude magnetic anomalies, the observed density and velocities favor the interpretation of an exhumed mantle (Figure 9A and Table 2).

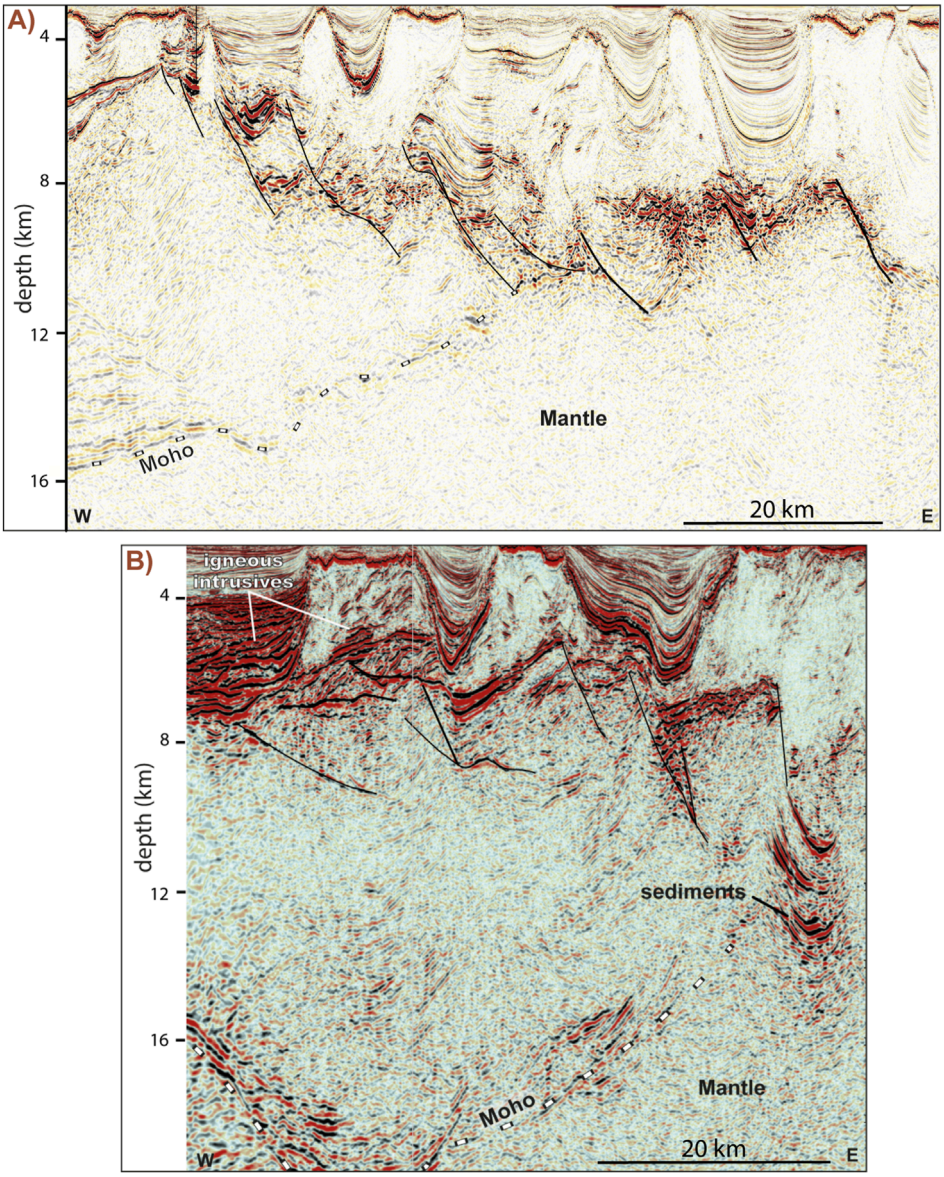

FIGURE 9
Details of 3D seismic lines within Zone IV (see location in Figures 1, 3B, 6B). Note the rise of the Moho reaching the base of chaotic sediments **(A)** and of a reflective sedimentary section **(B)**. Vertical exaggeration is 12 x.

Within the region of thickened crust (the OMR) the magnetic and gravity anomalies display high amplitudes and cannot be fit solely with continental crust, i.e., without massive magmatic additions. This is based on the fact that: 1) mafic/ultramafic igneous rocks are the most magnetic lithologies in the study area (and in general) (Lopes, 2023); 2) igneous intrusives exhibit strong reflectivity; and 3) the measured magnetic susceptibilities of the continental crust lithologies in southeast Brazil are generally low (Lopes, 2023).

Regarding the exhumed domain, the densities and magnetic anomalies are lower than those observed within the upper continental crust, the OMR and the crust at the hyperextended domain in the study area (Figure 6). The vertical gradient of the density is sharp and higher than that observed elsewhere, the seismic velocities are lower than continentward from the OMR and the overlying pre-salt section is distinct when compared to all other domains. Based on the previous and the observation of the Moho reflector shallowing and reaching the base of the sedimentary section (Figure 9), creating seawards a zone poorly reflective and without any visible Moho, it is unlikely that it constitutes an intruded crust. In that case, it would probably exhibit mild seismic reflectivity, higher magnetic signature, and densities comparable to the upper part of the OMR.

5 Interpretations

5.1 The deformation style at the distal and outer domains of the East Santos Basin

As proposed by several authors (e.g., Wernicke, 1985; Reynolds, 1985; Davis et al., 1983; Davis, 1986; Lister and Davis, 1983; Lister et al., 1984; Osmundsen et al., 2002; Duretz et al., 2016; Osmundsen et al., 2016), the extension of the crust and lithosphere may be accomplished by the combination of detachment faulting and ductile shear zones. In the study area, the Aquarius Detachment System (ADS) corresponds to upper crust low-angle to sub-horizontal listric faults, with the footwall crustal blocks highly back-tilted and isostatically uplifted, suggesting a mechanism of rolling-hinge (Buck et al., 1988), which led to the erosion of the pre-salt strata (Figures 3B, 5). The detachment faults changed shape passing eastward, becoming bowed up as thinning progressed. As that geometry of the faults was unsuited to accommodate displacement, it was transferred to structures located further east, resulting in deposition of progressively younger syn-kinematic strata oceanward. The large-scale horizontal displacement along the ADS led to the complete separation of the hanging wall from the footwall and the formation of supradetachment basins.

At the region of extreme upper crust thinning accomplished by the detachment system, deep reflectors at the lower crust are observed rising up and converging below the detachments (Figure 5) with an arched Moho, similar to the model of Block and Royden (1990) and the rolling-hinge model of Buck et al. (1988). The detachment faults seem to incise into the lower/intermediate reflective levels of the crust, similar to that observed at Basin and Range (Lister and Davis, 1989) and the Norwegian margin by Osmundsen et al. (2002). These authors and Fazlikhani et al. (2017) proposed that in hyperextended domains the lower crust can be pulled up by the deep-penetrating structures, flowing towards the faults footwalls, possibly indicating that the lower crustal deformation fabrics followed the upper crust deformational structures. The incising of the upper crust by lower crust shear zones was observed also by Osmundsen and Ebbing (2008), Peron-Pinvidic and Osmundsen (2016), at the South China Sea (Deng et al., 2020) and the Campos Basin (Alvarez et al., 2024). Lister and Davis (1989) envisaged that the basal shear zones observed below the detachments in the Basin and Range created mechanical conditions suitable for the nucleation and propagation of the upper detachments (a low viscosity layer), i.e., the upper and lower crust are extended and thinned together, characterizing a coupled deformation within the crust. This phenomenon is considered to result from the evolution from a crustal necking stage, when faults are expected to be decoupled from the mantle due to a lower crust deforming by ductile flow, to a hyperextension stage when the crust is less than 10 km thick, accompanied by the end of the ductile layers bringing the upper crust directly in contact with the subcontinental mantle (Brun and Beslier, 1996; Pérez-Gussinyé et al., 2001; Sutra and Manatschal, 2012; Frasca et al., 2016; Osmundsen and Peron-Pinvidic, 2018). Liu et al. (2022) modelled the interplay between brittle and ductile crustal deformation for several rifted margins exhibiting strong reflectors in the lower crust below detachment faults and concluded that these indicate a common mechanism of coupling processes. Duretz et al. (2016) modeled the deformation of a layered (inherited) lithosphere and proposed that in late rifting stages the weak material is significantly removed during thinning, allowing for the mechanical coupling of the crust and mantle lithosphere.

Based on a comparison with other rifted margins, the ADS constitutes an example of the type-HB1 high-B faults (coupling detachments, Osmundsen and Peron-Pinvidic, 2018), which include large-magnitude normal faults with planar, listric, or flat-ramp geometries, convex-upward, associated with footwall uplift, that promote lithosphere-scale deformation coupling (Mohn et al., 2012; Naliboff et al., 2017). The ADS marks a spatial change in the detachment surface geometry from concave-up to concave-down seaward, which created arched crustal blocks and fault splaying at some areas, similar to the flexural model of Block and Royden (1990) and Lavier and Manatschal (2006) and the rolling-hinge mechanism envisaged by Buck et al. (1988).

In that context, the isostatic response of the lithosphere may have allowed the fault surface, the Moho and the lithospheric mantle to flow upwards, leading to the exhumation of lower crust (Figures 2, 5) and the formation of a continental core-complex and the asthenospheric flow into the zone of extreme necking (Buck et al., 1988; Block and Royden, 1990). Such flow, in addition to the footwall uplift and denudation, and its incising by lower crust shear zones, probably changed the crustal rheology and its isostatic response to thinning, resulting in less subsidence of the hanging wall block (Lister and Davis, 1989). Moreover, the rise of upper mantle rocks to shallower depths may have induced adiabatic decompression melting, which could partially explain the ensuing formation of the OMR.

5.2 Formation of the aquarius detachment system and the outer magmatic ridge and consequences for lithospheric breakup

The distinct rifting styles observed in the CSB (inner necking breakaway complex) and ESB (outer necking breakaway complex) exerted a significant influence on the structural relief, tectonic style, and thickness of the post-rift and drift sequences. Although pre-salt carbonate rocks are imaged and sampled in both the CSB and the ESB, the structural relief of the base of salt (top of pre-salt carbonates) significantly varies across the Aquarius Lineament, deepening from ca. 4,500–6,500 m to 7,200–9,000 m at the ADS (based on De Freitas et al., 2022). This is coherent with major crustal thinning observed to the east of the ADS, which resulted in greater subsidence and accommodation space for the rift and drift sequences deposition (Figure 5) (De Freitas et al., 2022; Araujo et al., 2022).

The complex architecture observed at the distal Santos Basin documents successive tectonomagmatic stages. An initial distributed crustal stretching, with local basaltic intrusions and extrusions resulted in the creation of Zone I (Figures 3, 10). The formation of the ADS and abrupt crustal necking indicates that the deformation localized, resulting in intense thinning and creation of the hyperextended crust observed at Zone II. The low-energy pre-salt carbonate rocks of the sag sequence (Araujo et al., 2022) suggest an initial low topographic relief at this zone. During the thinning of

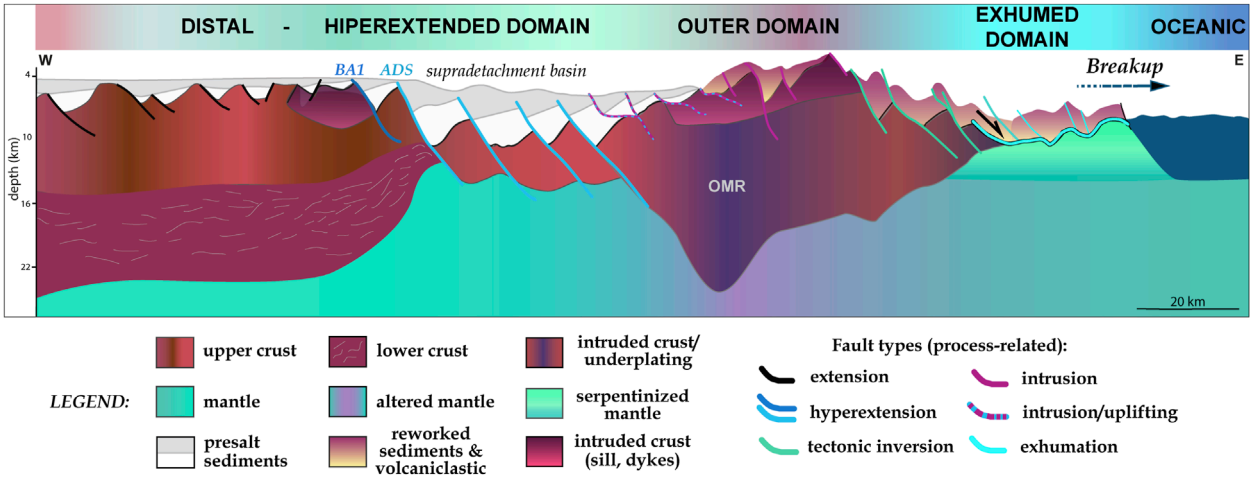

FIGURE 10
Sketched geological cross section in the central-east Santos hybrid margin (location in Figure 1) displaying the crustal structure and stratigraphy. The sedimentary section schematically represents only the pre-salt sequences. ADS- Aquarius Detachment System; BA1 e BA2 (ADS)- breakaway faults; OMR- Outer Magmatic R.idge.

the continental lithosphere, polyphase tectonic events commonly occur with varying magmatism concurrently with the rise of the asthenosphere. This condition naturally leads to increasing magma supply, which infiltrates the continental lithospheric mantle, ultimately resulting in the onset of the lithospheric breakup. In this last rifting stage, a magmatic pulse may form a volcanic edifice as observed in the West African and South China Sea margins (Gillard et al., 2016; Dong et al., 2020). This may explain the crust and pre-salt section at Zone III, where the stratigraphic sequence downlaps onto subhorizontal fault surfaces and exhibits top truncations marking a regional unconformity, pointing out the basement uplift, with a structural inversion of the syn-rift half grabens of the pre-salt section. This denotes the reactivation of a preexisting hyperextended crust. Alternatively, the crustal architecture of the ESB may also have been influenced by inherited structures and the transtensional and transpressional regimes associated with oblique rifting, leading to localized subsidence and uplift of crustal blocks, similar to the proposed mechanism for the São Paulo Plateau (Arnemann et al., 2023).

Based on the magnetic signature of continental basement rocks, the observation of strong magnetic and gravity anomalies, the thickened crust and distinctive reflective seismic facies within the OMR, a continental crust heavily intruded by igneous rocks seems to be the most probable lithology. Therefore, the evidence of tectonic reactivation within the OMR, combined with the thick and highly reflective crust observed at Zone III, argues for a magmatic push up causing the uplift of the original basement. We propose that the emplacement of massive magmatic additions progressively thickened the original crust through intrusives, extrusives, and underplating to create the OMR at Zone III. Such emplacement would have promoted uplift and tilting of the syn-rift half grabens, reactivating the faults up to the salt base (Figure 9). The eastern flank of the OMR exhibits large detachment faults that reach the mantle (Figure 3 Zone II), folded pre-salt sediments and compressive salt structures uplift, resulting from the elevated basement topography, which forming a barrier to the seaward salt migration (Figure 3 Zone III; Figure 7; Table 2).

The pre-salt section at Zone III includes intercalations with igneous extrusions (reported in Well 33) which may be immediately pre- or syn-tectonic to the emplacement of the OMR, since they are rotated and mixed with the carbonates. An age of ~120 Ma was proposed for the unconformity at the salt base and the breakup occurred at ~118 Ma (Alkmim et al., 2025).

The mechanism of magmatic emplacement leading to the crustal thickening was probably gradual, developed during successive volcanic pulses similar to that observed at the South China Sea (Dong et al., 2020). The ignition of the massive magmatism that created the OMR may be related to the abrupt crustal thinning in the hyperextended domain, resulting in the shallowing of the mantle isotherms (possibly accompanied by whole lithosphere thinning), increasing the adiabatic partial melting in the asthenosphere. Some studies have suggested the existence of a mantle thermal anomaly during the Cretaceous evolution of the Santos Basin (Ernesto, 2009; Carvas et al., 2021; Arnemann et al., 2023). These processes would have increased the magma supply, possibly leading to the emplacement of igneous rocks in the crust at deeper and shallower levels, with melts added to its base, building a large volcanic edifice. As a consequence, the emplaced material overthickened the original crust and modified its rheology and density structure, resulting in the uplift of the top basement and the tectonic inversion of the pre-salt strata observed at the ESB.

The crustal architecture and geophysical signature observed at the transition from a hyperextended crust at the ADS to the thickened crust forming the Outer Magmatic Ridge (OMR, Figure 7) implies a lateral change in the tectono-thermal regime within the outer margin, with a substantial increase in the volume of extrusive and intrusive rocks. The upper basement reflections possibly represent early flood basalts (Figures 3B, 7) similar to that observed at CSB Tupi Field (Gordon et al., 2023a), with syn-tectonic volcanics intercalated with low-energy carbonate rocks (Figure 8),

and widespread post- and intra-salt magmatic sills (Figure 3 Zones II and III and 9).

The OMR relative timing of formation can be tentatively established based on the pre-salt strata, the salt tectonics, and the deep crustal structure. The structural inversion of half-grabens and the compressional salt overlying it suggest that its emplacement was related to a late magmatic event (at the end of rifting). We propose that the original hyperextended crust presently at the OMR underwent deformation and thickenning through igneous intrusions/extrusions during final syn-rift and initial post-rift stages (between ca. 126–122 Ma, Alkmim et al., 2025), and probably was uplifted prior to salt deposition (120–119 Ma, Alkmim et al., 2025), mantle exhumation and continental breakup (c.a. 118–114 Ma, Alkmim et al., 2025). Nevertheless, it is necessary to date the igneous rocks of the OMR to properly constrain its age and evolution.

Similar ridge-shaped magnetic anomalies associated with magmatic edifices can be observed from seismic data at the outer domain of Santos Basin (Garcia et al., submitted), indicating that a stage of excess magmatism was not limited to the ESB and the OMR, but was possibly associated with a regional event (thermal anomaly?) at the end of rifting. At present there is no study to constrain this hypothesis, although at the southernmost portion of the São Paulo Plateau, earlier works have described thick volcanic successions overlying a thinned continental crust (Carminatti et al., 2008; Mohriak et al., 2008; Mohriak et al., 2010; Mohriak et al., 2007; Pindell et al., 2018; Arnemann et al., 2023). The Paraná-Etendeka LIP emplacement was pre-rift (Renne et al., 1996). However, the Santos Basin experienced recurrent magmatism during rift and drift stages (Gordon et al., 2023b), with alternations between magma-poor and magma-rich extensional episodes. Alternatively, the formation of a core-complex may indicate a high geothermal structure of the mantle during extension. According to Whitney et al. (2013) when the crust is very hot, the core-complex exhumation develops through detachment faulting accompanied by partial melting, favoring the flow of a low-viscosity lower crust. If that extension also involved necking of the entire lithosphere, the rising asthenosphere could increase the initial magmatic budget by adiabatic melting, resulting in an excess of magma. Deng et al. (2020) reported that the South China Sea margin displays large detachments that led to core-complex formation, followed by upper crust allochthons and finally by a volcanic edifice at the OCT.

The region eastward of the OMR displays distinct basement and stratigraphic characters (Figure 9). The top of the crust is not observed, and the basement is reflection-free in seismic data; the Moho rises up to the base of an unstructured sedimentary sequence that is overlain by massive salt. This evidence suggests that this region may correspond to a domain of exhumed mantle, an interpretation also proposed by Zalán et al. (2011). Considering the overlying apparently autochthonous salt (Figure 9), this domain possibly embodies a Zone of Exhumed Continental Mantle (ZECM), i.e., formed after crustal breakup but prior to lithospheric breakup and oceanic crust formation (observed to the east, see supplementary information) at ca. 118 Ma according to Alkmim et al. (2025). Therefore, after the formation of the OMR the magmatic supply seemed to have decreased and the final margin stage during salt deposition probably evolved under amagmatic conditions, without sufficient melt to promote breakup and formation of steady-state oceanic crust, resulting in the formation of a zone of exhumed continental mantle. Nevertheless, the proposed nature of this basement remains open to discussion without drilling data.

The observation of an outer volcanic structure and a potential zone of exhumed continental mantle at the outer Santos Basin indicates a distinctive tectonic, magmatic, and sedimentary final stage of evolution for this segment of the Brazilian margin, with possible impacts for the South American-African plate reconstructions and the pre-salt exploration. For instance, if the actual OMR structural high corresponds to a post-depositional basement uplift related to magmatic additions and isostatic compensation, the original pre-salt facies would have been deposited in distal locations rather than on structural highs similar to the Santos Basin giant fields Tupi, Mero, and Búzios which exhibit porous carbonate facies. As revealed by some wells in the distal margin of the Campos and Santos basins, the CO_2 content can reach over 90% by volume (Ferraz et al., 2019; Plawiak et al., 2024; De Freitas et al., 2022). Santos Neto et al. (2012) reported that such CO_2, and the C and He found in several hydrocarbon fields from pre-salt reservoirs in these basins have a mantle degassing origin. Some of the high CO_2 content areas exhibit detachment systems reaching the mantle, similar to the ADS (Juncken et al., 2024). Thus, the presence of large-scale deep faults, especially in zones of exhumed mantle, could have acted as conduits for the mantle fluids, H_2 and CO_2 migration to the pre-salt reservoirs. A possible exhumed mantle region has not been drilled yet, but fine-grained sediments, distal carbonate facies, abundant magmatic rocks, and fluids are expected in such zones (Pérez-Gussinyé et al., 2023), which do not represent favorable scenarios for oil prospecting.

5.3 Rifting transition from hyperextension to excess magmatism and to mantle exhumation: the formation of a hybrid margin

Rifted margins have been classified into magma-poor (MPM) and magma-rich (MRM) based on the timing and amount of extension and magmatism during their evolution (Geoffroy et al., 2015 and references therein). Nowadays there is a consensus that rifted margins are more complex and do not fit into simplistic categorizations. There are, however, first-order differences in the magmatic aspects within rifted margins. Generally, the MPM or less volcanic margins display a hyperextended crust and localized magmatism. Typical features may include large-scale listric and detachment fault systems creating break-away blocks (e.g., Boillot et al., 1980; Beslier et al., 1993; Whitmarsh et al., 1996; Pérez-Gussinyé et al., 2001; Reston, 2007; Peron-Pinvidic and Manatschal, 2009; Osmundsen et al., 2016; Gillard et al., 2016; Lymer et al., 2019), with possible mantle exhumation at the outer domain. Margins with abundant magmatism, generally called MRM (Eldholm et al., 1995; Larsen and Jakobsdóttir, 1988; White and Mckenzie, 1989; Keen and Potter, 1995; Reston and Manatschal, 2011; Franke, 2013) are usually marked by significant magmatic addition during rifting, often display SDRs (Seaward Dipping Reflectors, see Eldholm et al., 1995; Hinz, 1981; Mutter et al., 1982; Abreu, 1998; Talwani and

Abreu, 2000; White et al., 2008; Franke et al., 2010; Stica et al., 2014; McDermott et al., 2018), magmatic underplating, and a highly intruded lower crust (Geoffroy, 2005), and are frequently associated with Large Igneous Provinces (LIPs).

However, in the last decades, studies worldwide revealed that rifted margins are polyphase, exhibiting a wide range of tectonic and magmatic features formed in different stages during their evolution. The simple magma-rich/poor classification was combined with a weak/strong crust classification (based on the mechanical behavior of the crust) to account for the great complexity observed (Sapin et al., 2021 and references therein). The term "Hybrid" was proposed by Reston and Manatschal (2011) to describe margins that exhibit varying amounts of magmatism along strike. Peron-Pinvidic and Osmundsen (2018) highlighted that such hybrid margins sometimes display large amounts of crustal thinning prior to a "magmatic" breakup. Nonn et al. (2019) described the central Aden margin as a hybrid type due to unequal volcanic amounts between the conjugates, with the presence of SDRs and underplating at the more magmatic segment, and exhumed mantle at the less magmatic one. Pérez-Gussinyé et al. (2023) proposed another margin type named "Intermediate" which combines some of the elements of both endmembers, but lacks SDRs (or they are irrelevant) and exhumed mantle. The intermediate margins show significant magmatism, crustal thinning, and detachment structures at the distal and outer domains, with a typical example at the South China Sea margin.

The distal East Santos Basin exhibits singular first-order variations in crustal architecture and nature from west to east, with the transition from a moderately deformed to a hyperextended crust with deeply incising detachment faults reaching the mantle (Figure 10), followed by a thickened and highly intruded crust formed by excess magmatism in the late rifting stage (Figure 7), shifting to a domain where Moho rises suggesting mantle exhumation (Figure 9). With the exception of the last stage, the tectonomagmatic evolution of the ESB displays similarities with the adjacent Campos Basin: the extensional structures in the Distal Domain are also characterized by successive detachment faults, which resulted in the exhumation of the lower crust creating a continental core-complex (Alvarez et al., 2024), an outer magmatic ridge (Stanton et al., 2019) and a magmatic crust (Alvarez et al., 2024) prior to lithosphere breakup. Alternatively, the final crustal architecture at the ESB may have been influenced by transtension/compression tectonics at a late rifting stage. A comparison between the distal East Santos Basin and the conjugate Namibe Basin in the African margin (Escosa et al., 2024) show that the latter is much narrower but exhibits deformational structures similar to those reported here, including an exhumed mantle domain.

In summary, the Distal Domain of the East Santos Basin exhibits altogether the tectonic, magmatic and sedimentary elements that have previously been observed in magma-rich and magma-poor settings and thus is here interpreted as a "hybrid margin" (Figure 10). This type is distinct from the intermediate type proposed by Pérez-Gussinyé et al. (2023) where crustal and lithospheric thinning are accompanied by magma at shallower levels as dykes and underplated mafic rocks and culminate with lithospheric breakup and formation of "Penrose-like" oceanic crust. The hybrid margin of Santos does not clearly exhibit any evidence of magma at the hyperextended domain (Figures 3, 5). The magma came into the system after the process of hyperextension, as evidenced by the tectonic inversion of the Pre-salt faults and strata overlying the OMR during its formation. However, this magmatic pulse did not lead to lithospheric breakup and formation of oceanic crust, which is only observed to the east of the exhumed domain (see supplementary data). After the magmatic pulse the margin evolved to a later (amagmatic?) extensional stage, possibly exhuming the mantle. The transition from magmatic crust to mantle exhumation is difficult to reconcile, and further observations and models are necessary to unravel its mechanisms.

Remaining questions may include: What was the thermal evolution of the lithosphere during final rifting? What controlled the temporal, structural, and thermal variations?

6 Conclusions

- We document a regional structure named Aquarius Lineament and its associated ADS corresponding to N-S striking tectonic boundaries where first-order variations in crustal and stratigraphic architecture, structural style, and magmatism are observed, marking the limit between two contrasting margin segments: the Central Santos Basin and the East Santos Basin (ESB);
- The change in the structural style from concave-up to concave-down faults along the ADS generated arched crustal blocks and Moho, highly back-tilted footwall blocks and supradetachment basins that accommodated the thickest pre- and post-salt successions of the basin, coherent with the rolling-hinge mechanism of extension;
- At the ADS, deeply incising detachment faults reach the mantle and are reactivated, affecting the unconformity at the base of the sag, indicating that extensional deformation was active at least until ~122 Ma.
- The distal and outer domains of ESB exhibit architectural elements that highlight a distinct tectonic and thermal evolution of the lithosphere during final rifting, transitioning from: 1) distributed crustal thinning; 2) hyperextension with the breakup of the lower crust without evidence of magma; 3) excess magmatism, deforming the originally hyperextended crust, generating a thick and highly intruded crust and underplating; 4) mantle exhumation; 5) lithospheric breakup at ca. 118 Ma based on published ages. The observed crustal architecture may also have been influenced by the transtensional tectonics related to the oblique rift kinematics at the study area.
- We document for the first time a late-rift to early post-rift tectonomagmatic event at the outer ESB, resulting in massive magmatic additions and underplating, forming an Outer Magmatic Ridge. Its emplacement promoted basement uplift, inverting the syn-rift half grabens, reactivating faults at the salt base, and creating pop up basement structures. A relative age (based on published data) for the formation of this feature is proposed approximately between 126 and 121 Ma.
- Our observations suggest the existence of an exhumed continental mantle domain at the most distal part of the ESB,

with implications for the South Atlantic plate reconstructions and the pre-salt exploration.
- Several similarities with the tectonomagmatic evolution of the adjacent Campos Basin can be highlighted, such as the existence of extensional structures in the Distal Domain controlled by successive detachment faults leading to the exhumation of deeper levels of crust and mantle, and the formation of an outer magmatic ridge.

Data availability statement

The data analyzed in this study is subject to the following licenses/restrictions: The seismic data is proprietary. Requests to access these datasets should be directed to secretaria_sdt@anp.gov.br.

Author contributions

NS: Conceptualization, Data curation, Formal Analysis, Investigation, Methodology, Validation, Visualization, Writing – original draft, Writing – review and editing. AG: Conceptualization, Data curation, Formal Analysis, Investigation, Validation, Visualization, Writing – original draft, Writing – review and editing.

Funding

The author(s) declare that financial support was received for the research and/or publication of this article. Natasha Stanton acknowledges FAPERJ for the APQ1 grants number SEI-260003/015458/2021.

Acknowledgments

The authors are grateful to the reviewers Alessandro Decarlis, Chris Morley, Mohamed Gouiza and Charlotte Nielsen for their detailed and thoughtful comments on a previous version of the text, and to two reviewers that helped to improve the manuscript. The CGG (now Viridien) is thanked for the permission to publish the seismic data. Natasha Stanton acknowledges the ANP for the public data.

Conflict of interest

The authors declare that the research was conducted in the absence of any commercial or financial relationships that could be construed as a potential conflict of interest.

Generative AI statement

The author(s) declare that no Generative AI was used in the creation of this manuscript.

Any alternative text (alt text) provided alongside figures in this article has been generated by Frontiers with the support of artificial intelligence and reasonable efforts have been made to ensure accuracy, including review by the authors wherever possible. If you identify any issues, please contact us.

Publisher's note

Supplementary material

The Supplementary Material for this article can be found online at: https://www.frontiersin.org/articles/10.3389/feart.2025.1665965/full#supplementary-material

References

Abreu, V. S. (1998). "Geologic evolution of conjugate volcanic passive margins: Pelotas basin (brazil) and offshore Namibia (africa)," in *Implication for global sea-level changes*. Houston, Texas: Rice University, 354. Available online at: https://scholarship.rice.edu/handle/1911/19338.

Alkmim, F. F., Lana, C. C., Silva, M. A., Dias-Filho, D. C., Mendonça, K. R., Zambonato, E. E., et al. (2025). U-Pb ages of pre-to post-salt carbonates, santos and campos basins, SE Brazil: implications for the evolution of the south Atlantic. *Mar. Petroleum Geol.* 171, 107192. doi:10.1016/j.marpetgeo.2024.107192

Alvarez, P., Stanton, N., Peron-Pinvidic, G., Magnavita, L., and Borghi, L. (2024). Crustal architecture and magmatism of the campos rifted margin: along-strike variability and segmentation. *Tectonics* 43, e2024TC008424. doi:10.1029/2024TC008424

Araujo, M. N., Pérez-Gussinyé, M., and Mushaldev, I. (2022). *Oceanward rift migration during formation of santos-benguela ultra-wide rifted margin*, 524. Geological Society, London, Special Publications.

Arnemann, M., Abreu, V., Rostirolla, S., and Barboza, E. (2023). Lateral changes of crustal extension and passive margin type along the Brazilian southeastern margin. *J. Sea Res.* 196, 102459–25. doi:10.1016/j.seares.2023.102459

Asmus, H. E., and Ponte, F. C. (1973). "The Brazilian marginal basins," in *The ocean basins and margins 1: the south Atlantic*. Editors A. E. Nair, and F. G. Stehli (New York: Springer, Plenum Press).

Autin, J., Bellahsen, N., Leroy, S., Husson, L., Beslier, M.-O., and d'Acremont, E. (2013). The role of structural inheritance in oblique rifting: insights from analogue models and application to the gulf of Aden. *Tectonophysics* 607, 51–64. doi:10.1016/j.tecto.2013.05.041

Baranov, V. (1957). A new method for interpretation of aeromagnetic maps: pseudo-gravimetric anomalies. *Geophysics* 22, 359–382. doi:10.1190/1.1438369

Baranov, V., and Naudy (1964). Numerical calculation of the formula of reduction to the magnetic pole. *Geophysics* 29, 67–79. doi:10.1190/1.1439334

Beniest, A., Willingshofer, E., Sokoutis, D., and Sassi, W. (2018). Extending Continental lithosphere with lateral strength variations: effects on deformation localization and margin geometries. *Front. Earth Sci.* 6 (6), p148. doi:10.3389/feart.2018.00148

Beslier, M. O., Ask, M., and Boillot, G. (1993). "Ocean-continent boundary in the iberia abyssal plain from multichannel seismic data,", 218. Amsterdam, 383–393. doi:10.1016/0040-1951(93)90327-g*Tectonophysics*

Block, L., and Royden, L. H. (1990). Core complex geometries and regional scale flow in the lower crust. *Tectonics* 9 (4), 557–567. doi:10.1029/tc009i004p00557

Boillot, G., Grimaud, S., Mauffret, A., Mougenot, D., Kornprobst, J., Mergoil-Daniel, J., et al. (1980). "Ocean-continent boundary off the Iberian margin: a serpentinite diapir west of the Galicia bank,", 48. Amsterdam, 23–34. doi:10.1016/0012-821x(80)90166-1*Earth and Planet. Sci. Lett.*

Brun, J. P., and Beslier, M. O. (1996). Mantle exhumation at passive margins. *Earth Planet. Sc. Lett.* 142, 161–173. doi:10.1016/0012-821x(96)00080-5

Brune, S. (2016). "Rifts and rifted margins," in *Plate boundaries and natural hazards*. Editors J. C. Duarte, and W. P. Schellart doi:10.1002/9781119054146.ch2

Brune, S., Kolawole, F., Olive, J.-A., Sarah Stamps, D., Buck, R., Buiter, S. J. H., et al. (2023). Geodynamics of Continental rift initiation and evolution. *Nat. Rev. Earth and Environ.* 4 (4), 235–253. doi:10.1038/s43017-023-00391-3

Buck, W. R., Martinez, F., Steckler, M. S., and Cochran, J. R. (1988). Thermal consequences of lithospheric extension: pure and simple. *Tectonics* 7 (2), 213–234. doi:10.1029/TC007i002p00213

Candeias, F., Mohriak, W. U., Porto, A., and Gordon, A. C. (2024). The impact of the abimael ridge on the salt tectonics in the southern santos Basin, Brazil: the esmeralda exploration block case. *J. S. Am. Earth Sci.* 148, 105094. doi:10.1016/j.jsames.2024.105094

Capistrano, G. G., Schmitt, R. S., Medeiros, S. R., and Vieira, T. A. T. (2021). Ediacaran ophiolite relics in the SE Brazilian Coast: field, geochemical and geochronological evidence from metabasites and paragneisses. *J. S. Am. Earth Sci.* 105, 103040. doi:10.1016/j.jsames.2020.103040

Cappelletti, A., Tsikalas, F., Nestola, Y., Cavozzi, C., Argnani, A., Meda, M., et al. (2013). Impact of lithospheric heterogeneities on Continental rifting evolution: constraints from analogue modelling on south Atlantic margins. *Tectonophysics* 608, 30–50. doi:10.1016/j.tecto.2013.09.026

Carmichael, R. S. (1982). *Magnetic properties of minerals and rocks: practical handbook of physical properties of rocks and minerals*. 1st ed. CRC Press.

Carminatti, M., Wolff, B., and Gamboa, L. (2008). "New exploratory frontiers in Brazil," in *Paper presented at the 19th world petroleum congress*.

Carmo, I. O., Schmitt, R., Araújo, M. N. C., and Romeiro, M. A. T. (2017). "Evidence for the paleoproterozoic/cambrian Angolan belt in the Brazilian margins – new data from offshore basement drill core," in *Abstract 5th conjugate margins conference. August 2017*. Porto de Galinhas, Pernambuco, Brazil.

Carvas, K. Z., Vasconcelos, P. M. P., Marques, L. S., Ubide, T., Carmo, I. O., and Babinski, M. (2021). Geochronology of mafic magmatism and hydrothermal alteration during early stages of south Atlantic opening. *Geochimica Cosmochimica Acta* 314, 358–380. doi:10.1016/j.gca.2021.08.017

Chang, H. K., Kowsmann, R. O., Figueiredo, A. M. F., and Bender, A. (1992). Tectonics and stratigraphy of the east Brazil rift system: an overview. *Tectonophysics* 213, 97–138. doi:10.1016/b978-0-444-89912-5.50032-6

Corti, G., Ranalli, G., Mulugeta, G., Agostini, A., Sani, F., and Zugu, A. (2010). Control of the rheological structure of the lithosphere on the inward migration of tectonic activity during Continental rifting. *Tectonophysics* 490, 165–172. doi:10.1016/j.tecto.2010.05.004

Davis, G. A. (1986). Upward transport of mid-crustal mylonitic gneisses in the footwall of a Miocene detachment fault,whipple Mountains, southeastern California. *Geol. Soc. Am. Abs.* 18, 98.

Davis, G. A., Lister, G. S., and Reynolds, S. J. (1983). Interpretation of Cordilleran core complexes as evolving crustal shear zones in an extending orogen. *Geol. Soc. Am. Abs.* 12, 311.

De Freitas, V. A., dos Santos Vital, J. C., Rodrigues, B. R., and Rodrigues, R. (2022). Source rock potential, main depocenters, and CO2 occurrence in the pre-salt section of santos basin, southeast Brazil. *J. S. Am. Earth Sci.* 115, 103760. doi:10.1016/j.jsames.2022.103760

Dean, S. M., Minshull, T. A., Whitmarsh, R. B., and Louden, K. E. (2000). Deep structure of the ocean-continent transition in the southern iberia abyssal plain from seismic refraction profiles: the IAM-9 transect at 40°20′N. *J. Geophys. Res.* 105, 5859–5885. doi:10.1029/1999jb900301

Decarlis, A., Gillard, M., Tribuzio, R., Epin, M. E., and Manatschal, G. (2018). Breaking up continents at magma-poor rifted margins: a seismic V. Outcrop perspective. *J. Geol. Soc.* 175 (6), 875–882. doi:10.1144/jgs2018-041

Deng, H., Ren, J., Pang, X., Rey, P. F., McClay, K. R., Watkinson, I. M., et al. (2020). South China Sea documents the transition from wide Continental rift to Continental break up. *Nat. Commun.* 11, 4583. doi:10.1038/s41467-020-18448-y

Dong, S. W., Li, J. H., Cawood, P. A., Gao, R., Zhang, Y. Q., and Xin, Y. J. (2020). Mantle influx compensates crustal thinning beneath the Cathaysia Block, south China: evi-dence from SINOPROBE reflection profiling. *Earth Planet. Sci. Lett.* 544, 116360. doi:10.1016/j.epsl.2020.116360

Duretz, T., Petri, B., Mohn, G., Schmalholz, S. M., Schenker, F. L., and Müntener, O. (2016). The importance of structural softening for the evolution and architecture of passive margins. *Sci. Rep.* 6, 38704. doi:10.1038/srep38704

Eldholm, O., Skogseid, J., Planke, S. K., and Gladczenko, T. (1995). "Volcanic margin concepts," in *Rifted ocean-continent boundaries*. Editors E. Banda, M. Torne, and M. Talwani (Dordrecht: Kluwer Academic Publishers), 1–16.

Ernesto, M. (2009). Contribuições dos estudos paleomagnéticos ao entendimento da abertura do Atlantico. *Bol. De. GEOCIÊNCIAS DA PETROBRAS (IMPRESSO)* 17, 353–363.

Escosa, F. O., Denis, M., Nielsen, C., Ringenbach, J. C., and Guiraud, M. (2024). Mode of extension and final architecture of the south Angolan margins controlled by Precambrian lithospheric heterogeneity. *Mar. Petroleum Geol.* 161, 106637. doi:10.1016/j.marpetgeo.2023.106637

Evain, M., Afilhado, A., Rigoti, C., Loureiro, A., Alves, D., Klingelhoefer, F., et al. (2015). Deep structure of the santos basinsão paulo Plateau system, SE Brazil. *J. Geophys. Res. Solid Earth* 120 (8), 5401–5431. doi:10.1002/2014jb011561

Fazlikhani, H., Fossen, H., Gawthorpe, R. L., Faleide, J. I., and Bell, R. E. (2017). Basement structure and its influence on the structural configuration of the northern north sea rift. *Tectonics* 36, 6, 1151–1177. doi:10.1002/2017TC004514

Feng, M., van der Lee, S., and Assumpcão, M. (2007). Upper mantle structure of South America from joint inversion of waveforms and fundamental mode group velocities of rayleigh waves. *J. Geophys. Res.* 112, B04312. doi:10.1029/2006JB004449

Ferraz, A., Gamboa, L., dos Santos Neto, E. V., and Baptista, R. (2019). Crustal structure and CO2 occurrences in the Brazilian basins. *Interpretation* 7 (4), SL37–SL45. doi:10.1190/int-2019-0038.1

Ferreira, L. C., Stanton, N., Gordon, A. C., and Schmitt, R. (2023). The magmatic rifting of santos basin: aeromagnetic mapping of dykes, terranes and marginal structures and the interplay between tectonism and volcanism. *Tectonics* 42, e2022TC007560. volume42, number 4. doi:10.1029/2022TC007560

Franke, D. (2013). Rifting, lithosphere breakup and volcanism: comparison of magma-poor and volcanic rifted margins. *Mar. Petroleum Geol.* 43, 63–87. doi:10.1016/j.marpetgeo.2012.11.003

Franke, D., Ladage, S., Schnabel, M., Schreckenberger, B., Reichert, C., Hinz, K., et al. (2010). Birth of a volcanic margin off Argentina, south Atlantic. *Geochem. Geophys. Geosystems* 11, 2009GC002715. doi:10.1029/2009gc002715

Frasca, G., Gueydan, F., Brun, J. P., and Monié, P. (2016). Deformation mechanisms in a Continental rift up to mantle exhumation. Field evidence from the Western betics, Spain. *Mar. Petroleum Geol.* 76, 310–328. doi:10.1016/j.marpetgeo.2016.04.020

Geoffroy, L. (2005). "Volcanic passive margins,", 337. Amsterdam, 1395–1408. doi:10.1016/j.crte.2005.10.006*Geoscience*

Geoffroy, L., Burov, E., and Werner, P. (2015). Volcanic passive margins: another way to break up continents. *Sci. Rep.* 5, 14828. doi:10.1038/srep14828

Gillard, M., Autin, J., and Manatschal, G. (2016). Fault systems at hyper-extended rifted margins and embryonic Oceanic crust: structural style, evolution and relation to magma. *Mar. Pet. Geol.* 76, 51–67. doi:10.1016/j.marpetgeo.2016.05.013

Gomes, P. O., Kilsdonk, B., Minken, J., Grow, T., and Barragan, R. (2009). "The outer high of the santos basin, southern São Paulo Plateau, Brazil: pre-salt exploration outbreak, paleogeographic setting, and evolution of the syn-rift structures," in *AAPG international conference and exhibition*, 15–18.

Gordon, A. C., Mohriak, W. U., Stanton, N., and Santos, A. C. (2023a). Magmatic cycles in santos basin (SE Brazil): tectonic control in the temporal-spatial distribution and geophysical signature. *J. S. Am. Earth Sci.* 121, 104111. doi:10.1016/j.jsames.2022.104111

Gordon, A. C., Santos, A. C., Caitano, G. R., Stanton, N., and Mohriak, W. U. (2023b). Magmatic cycles in Santos basin (SE Brazil): geochemical characterization and magmatic sources. *J. S. Am. Earth Sci.* 126, 104323. doi:10.1016/j.jsames.2023.104323

Gouiza, M., and Naliboff, J. (2021). Rheological inheritance controls the formation of segmented rifted margins in cratonic lithosphere. *Nat. Commun.* 12 v. 1, 4653–53. doi:10.1038/s41467-021-24945-5

Haas, P., Müller, R. D., Ebbing, J., Finger, N.-P., Kaban, M. K., and Heine, C. (2022). Modeling lithospheric thickness along the conjugate south Atlantic passive margins implies asymmetric rift initiation. *Tectonics* 41, e2021TC006828. doi:10.1029/2021TC006828

Heilbron, M., Mohriak, W., Valeriano, C. M., Milani, E., Almeida, J. C. H., and Tupinamba, M. (2000). "From collision to extension: the roots of the south-eastern Continental margin of Brazil," in *Atlantic rifts and Continental margins. Geophysical monographs*. Editors M. Talwani, and W. Mohriak (American Geophysical Union), 115, 1–32. doi:10.1029/gm115p0001

Hinz, K. A. (1981). Hypothesis on terrestrial catastrophes: wedges of very thick ocean ward dipping layers beneath passive Continental margins-their origin, and paleoenvironmental significance. *Geol. Jahrb. Reihe E, Geophys.* 22, 3–28.

Huang, R., Zhang, Z., Wu, Z., Wei, Z., Mei, J., and Wang, P. (2021). Full-waveform inversion for full-wavefield imaging: decades in the making. *Lead. Edge* 40 (5), 324–334. doi:10.1190/tle40050324.1

Huismans, R., and Beaumont, C. (2011). Depth-dependent extension, two-stage breakup and cratonic underplating at rifted margins. *Nature* 473, 74–78. doi:10.1038/nature09988

Juncken, R., Lyra, B., Gatti, M., Stanton, N., and Gordon, A. (2024). Santos basin: new seismic data helps de-risk CO2 contamination for pre-salt exploration. *GeoExPro online Mag.*, 48–50.

Karner, G. D. (2000). "Rifts of the campos and santos basins," in *Southeastern Brazil: distribution and timing*, 73. AAPG Memoir. Chapter 21.

Karner, G. D., Johnson, C., Shoffner, J., Lawson, M., Sullivan, M., Sitgreaves, J., et al. (2021). "Chapter 9: tectono-magmatic development of the santos and campos basins, offshore Brazil,". *Tectono-magmatic development of the santos and campos basins, offshore Brazil. In the supergiant Lower Cretaceous pre-salt petroleum systems of the santos basin, Brazil*. Editors M. Rocha Mello, P. Oya Yilmaz, and B. J. Katz (The American Association of Petroleum Geologists and Brazil petrostudies, Memoir), 124, 215–256. doi:10.1306/13722321MSB.9.1853

Keen, C. E., and Potter, D. P. (1995). The transition from a volcanic to a nonvolcanic rifted margin off eastern Canada. *Tectonics* 14, 359–371. doi:10.1029/94tc03090

King, M. T., and Welford, J. K. (2022). *Advances in deformable plate tectonic models: 1. Reconstructing deformable Continental blocks and crustal thicknesses back through time*, G3, 23.

Kumar, N., Danforth, A., Nuttall, P., Helwig, J., Bird, D. E., and Venkatraman, S. (2013). From Oceanic crust to exhumed mantle: a 40 year (1970–2010) perspective on the nature of crust under the santos basin, SE Brazil. *Geol. Soc. Lond. Spec. Publ.* 369 (1), 147–165. doi:10.1144/sp369.16

Kusznir, N. J., and Park, R. G. (1987). The extensional strength of the Continental lithosphere: its dependence on geothermal gradient, and crustal composition and thickness. *Geol. Soc. Lond. Spec. Publ.* 28, 35–52. doi:10.1144/GSL.SP.1987.028.01.04

Larsen, H. C., and Jakobsdóttir, S. (1988). "Distribution, crustal properties and significance of seawards-dipping sub-basement reflectors off E Greenland, in morton,". *Early tertiary volcanism and the opening of the NE Atlantic*. Editor L. M. Parson (London: Geological Society), 39, 95–114.

Lavier, L. L., and Manatschal, G. (2006). A mechanism to thin the Continental lithosphere at magma-poor margins. *Nature* 440 (7082), 324–328. doi:10.1038/nature04608

Lavier, L., Buck, W. R., and Poliakov, A. N. B. (1999). Self-consistent rolling Hinge model for the evolution of large-offset low-angle normal faults. *Geology* 27 (12), 1127–1130. doi:10.1130/0091-7613(1999)027<1127:scrhmf>2.3.co;2

Lavier, L. L., Buck, W. R., and Poliakov, A. N. B. (2000). Factors controlling normal fault offset in an ideal brittle layer. *J. Geophys. Res.* 105 (B10), 23431–23442. doi:10.1029/2000JB900108

Leroy, S., Gente, P., Fournier, M., D'Acremont, E., Patriat, P., Beslier, M.-O., et al. (2004). From rifting to spreading in the eastern gulf of Aden: a geophysical survey of a young Oceanic basin from margin to margin. *Terra nova.* 16, 185–192. doi:10.1111/j.1365-3121.2004.00550.x

Lister, G. S., and Davis, G. A. (1983). Development of mylonitic rocks in an intracrustal laminar flow zone, whipple Mountains, SE California. *Geol. Soc. Am. Abs.* 12, 310.

Lister, G. S., and Davis, G. A. (1989). "The origin of metamorphic core complexes and detachment faults formed during tertiary Continental extension in the northern colorado river region, U.S.A,", 11. Amsterdam, 65–94. doi:10.1016/0191-8141(89)90036-9*J. Struct. Geol.*

Lister, G. S., Banga, G., and Feenstra, A. (1984). Metamorphic core complexes of Cordilleran type in the cyclades, aegean sea, Greece. *Geology* 12, 221–225. doi:10.1130/0091-7613(1984)12<221:mccoct>2.0.co;2

Lister, G. S., Etheridge, M. A., and Symonds, P. A. (1986). Detachment faulting and the evolution of passive Continental margins. *Geology* 14, 246–250. doi:10.1130/0091-7613(1986)14<246:dfateo>2.0.co;2

Liu, X., Fu, X., Liu, D., Wei, W., Lu, X., Liu, C., et al. (2018). Distribution of mantle-derived CO2 gas reservoir and its relationship with basement faults in songliao Basin, China. *J. Nat. Gas Sci. Eng.* 56, 593–607. doi:10.1016/j.jngse.2018.06.040

Liu, Z., Pérez-Gussinyé, M., Rüpke, L., Muldashev, I. A., Minshull, T. A., and Bayrakci, G. (2022). Lateral coexistence of ductile and brittle deformation shapes magma-poor distal margins: an example from the west iberia-newfoundland margins. *Earth Planet. Sci. Lett.* 578, 117288. doi:10.1016/j.epsl.2021.117288

Lopes, R. (2023). *Prolongamento offshore da sutura cambriana entre o Domínio Tectônico do Cabo Frio e o Terreno Oriental: uma descontinuidade do embasamento proximal da bacia de Santos*. Brazil: Federal University of Rio de Janeiro, 122. MsC thesis.

Lymer, G., Cresswell, D. J. F., Reston, T. J., Bull, J. M., Sawyer, D. S., Morgan, J. K., et al. (2019). 3D development of detachment faulting during Continental breakup. *Earth Planet. Sc. Lett.* 515, 90–99. doi:10.1016/j.epsl.2019.03.018

Martins, G. G., Mendes, J. C., Schmitt, R. S., and Armstrong, R. (2021). Unravelling source and tectonic environment of an Ediacaran magmatic province from southeast Brazil: insights from geochemistry and isotopic investigation. *Lithos*, 106428–405. doi:10.1016/j.lithos.2021.106428

Masini, E., Manatschal, G., Mohn, G., Ghienne, J.-F., and Lafont, F. (2011). The tectono sedimentary evolution of a supradetachment rift basin at a deep-water magma-poor rifted margin: the example of the samedan basin preserved in the err nappe in SE Switzerland. *Basin Res.* 23, 652–677. doi:10.1111/j.1365-2117.2011.00509.x

McDermott, C., Lonergan, L., Collier, J. S., McDermott, K. G., and Bellingham, P. (2018). Characterization of seaward-dipping reflectors along the south American Atlantic margin and implications for Continental breakup. *Tectonics* 37, 3303–3327. doi:10.1029/2017TC004923

McKenzie, D. P. (1978). Some remarks on the development of sedimentary basins. *Earth Planet. Sci. Lett.* 40, 25–32. doi:10.1016/0012-821X(78)90071-7

Meyer, B., Chulliat, A., and Saltus, R. (2017). Derivation and error analysis of the Earth magnetic anomaly grid at 2 arc min resolution version 3 (EMAG2v3). *Geochem. Geophys. Geosystems* 18, 4522–4537. doi:10.1002/2017GC007280

Miller, D. J., and Christensen, N. I. (1999). Seismic velocities of lower crustal and upper mantle rocks from the slow-spreading mid-atlantic ridge, south of the kane transform (MARK). *Proc. Ocean. Drill. Program Sci. Results* 153, 437–454.

Minty, B. R. S., and Luyendyk, A. P. J. (1997). Brodie calibration and data processing for airborne gamma ray spectrometry AGSO. *J. Aust. Geol. Geophys.* 17 (2), 51–62.

Mohn, G., Manatschal, G., Beltrando, M., Masini, E., and Kusznir, N. (2012). Necking of Continental crust in magma poor rifted margins: evidence from the fossil alpine tethys margins. *Tectonics* 31, TC1012. doi:10.1029/2011TC002961

Mohriak, W. U. (2001). "Salt tectonics, volcanic centers, fracture zones and their relationship with the origin and evolution of the south Atlantic Ocean: geophysical evidence in the Brazilian and West African margins," in *7th international congress of the Brazilian geophysical society, salvador, Bahia, expanded abstract*, 1594–1597.

Mohriak, W. U. (2003). "Bacias Sedimentares da Margem Continental Brasileira,". *Geologia, Tectônica e Recursos Minerais do Brasil*. Editors L. A. Bizzi, C. Schobbenhaus, R. M. Vidotti, and J. H. Gonçalves (CPRM), III. Capítulo.87165

Mohriak, W. U., Rosendahl, B. R., Turner, J. P., and Valente, S. C. (2002). "Crustal architecture of south Atlantic volcanic margins," in *Volcanic rifted margins*. Editors M. A. MENZIES, S. L. KLEMPERER, C. J. EBINGER, and J. BAKER (Boulder, Colorado: Geological Society of America.), 159–202.

Mohriak, W. U., Nemcok, M., and Enciso, G. (2008). "South Atlantic divergent margin evolution: rift-border uplift and salt tectonics in the basins of SE Brazil,". *West gondwana pre-cenozoic correlations across the south Atlantic region*. Editors R. J. Pankhurst, R. A. J. Trouw, B. B. Brito Neves, and M. J. de Wit (Geological Society, London, Special Publications), 294, 365–398. doi:10.1144/SP294.19

Mohriak, W. U., Nóbrega, M., Odegard, M. E., Gomes, B. S., and Dickson, W. G. (2010). Geological and geophysical interpretation of the rio grande rise, south-eastern Brazilian margin: extensional tectonics and rifting of continental and Oceanic crusts. *Pet. Geosci.* 16 (3), 231–245. doi:10.1144/1354-079309-910

Moreira, J. L. P., Madeira, C. V., Gil, J. A., and Machado, M. A. P. (2007). Bacia de Santos. *Bol. Geociências PETROBRAS* 15 (2), 531–549.

Moulin, M., Aslanian, D., Rabineau, M., Patriat, M., and Matias, L. (2013). "Kinematic keys of the santos–namibe basins,", 369. London, Special Publications, 91–107. doi:10.1144/sp369.3*Geol. Soc.*1

Mutter, J., Talwani, M., and Stoffa, K. (1982). "Origin of seaward-dipping reflectors in Oceanic crust off the Norwegian margin by "subaerial seafloor spreading"",*Geology*, 10. Washington, 353–357. doi:10.1130/0091-7613(1982)10<353:oosrio>2.0.co;2

Naliboff, J., and Buiter, S. J. H. (2015). Rift reactivation and migration during multiphase extension. *Earth Planet. Sci. Lett.* 421, 58–67. doi:10.1016/j.epsl.2015.03.050

Naliboff, J., Buiter, S. J. H., Péron-Pinvidic, G., Osmundsen, P. T., and Tetrault, J. (2017). Complex fault interaction controls Continental rifting. *Nat. Commun.* 8 (1), 1179. doi:10.1038/s41467-017-00904-x

Nonn, C., Leroy, S., Lescanne, M., and Castilla, R. (2019). Central gulf of Aden conjugate margins (Yemen-Somalia): tectono-Sedimentary and magmatism evolution in hybrid-type margins. *Mar. Petroleum Geol.* 105, 100–123. doi:10.1016/j.marpetgeo.2018.11.053

Osmundsen, P. T., and Ebbing, J. (2008). Styles of extension offshore mid-Norway and implications for mechanisms of crustal thinning at passive margins. *Tectonics* 27, TC6016. doi:10.1029/2007TC002242

Osmundsen, P. T., and Peron-Pinvidic, G. (2018). Crustal-scale fault interaction at rifted margins and the formation of domain-bounding breakaway complexes: insights from offshore Norway. *Tectonics* 37 (3), 935–964. doi:10.1002/2017tc004792

Osmundsen, P. T., Sommaruga, A., Skilbrei, J. R., and Olesen, O. (2002). Deep structure of the mid-Norway rifted margin, norw. *J. Geol.* 82, 205–224.

Osmundsen, P. T., Peron-Pinvidic, G., Ebbing, J., Erratt, D., Fjellanger, E., Bergslien, D., et al. (2016). Extension, hyperextension and mantle exhumation offshore Norway: a discussion based on 6 crustal transects. *Nor. J. Geol.* 96. doi:10.17850/njg96-4-05

Pérez-Gussinyé, M., and Reston, T. J. (2001). Rheological evolution during extension at nonvolcanic rifted margins: onset of serpentinization and development of detachments leading to Continental breakup. *J. Geophys. Res. B Solid Earth* 106, 3961–3975. doi:10.1029/2000jb900325

Pérez-Gussinyé, M. P., Reston T, J., and Morgan, J. P. (2001). "Serpentinization and magmatism during extension at non-volcanic margins: the effect of the initial

lithospheric structure,". *Non-volcanic rifting of Continental margins: a comparison of evidence from land and sea*. Editors R. C. L. WILSON, R. B. WHITMARSH, B. TAYLOR, and N. FROITZHEIM (London: Geological Society: Special Publications), 187, 511–536.

Pérez-Gussinyé, M., Collier, J. S., Armitage, J. J., Hopper, J. R., Sun, Z., and Ranero, C. R. (2023). Towards a process-based understanding of rifted Continental margins. *Nat. Rev. Earth and Environ.* 4 (3), 166–184. doi:10.1038/s43017-022-00380-y

Peron-Pinvidic, G., and Manatschal, G. (2009). "The final rifting evolution at deep magma-poor passive margins from iberia-newfoundland: a new point of view,"*Int. J. Earth Sci. (Geol Rundsch)*, 98. Heidelberg, 1581–1597. doi:10.1007/s00531-008-0337-9

Peron-Pinvidic, G., and Osmundsen, P. T. (2016). Architecture of the distal and outer domains of the mid-norwegian rifted margin: insights from the rån-gjallar ridges system. *Mar. Petroleum Geol.* 77, 280–299. doi:10.1016/j.marpetgeo.2016.06.014

Peron-Pinvidic, G., and Osmundsen, P. T. (2018). The mid Norwegian - NE Greenland conjugate margins: rifting evolution, margin segmentation, and breakup. *Mar. Petroleum Geol.* 98, 162–184. doi:10.1016/j.marpetgeo.2018.08.011

Peron-Pinvidic, G., Manatschal, G., and Osmundsen, P. T. (2013). Structural comparison of archetypal Atlantic rifted margins: a review of observations and concepts. *Mar. Pet. Geol.* 43, 21–47. doi:10.1016/j.marpetgeo.2013.02.002

Pindell, J., Graham, R., and Horn, B. W. (2018). "Role of outer marginal collapse on salt deposition in the eastern Gulf of Mexico, campos and santos basins,". Editors K. R. McClay, and J. A. Hammerstein (Geological Society, London, Special Publications), 476, 317–331. doi:10.1144/SP476.4*Passive Margins Tect. Sediment. Magmatism*

Plawiak, R. A. B., Carvalho, M. J., Sombra, C. L., Brandão, D. R., Mepen, M., Ferrari, A. L., et al. (2024). Structural controls of the migration of mantle-derived CO2 offshore in the santos basin (southeastern Brazil). *Front. Earth Sci.* 11, 1284151. doi:10.3389/feart.2023.1284151

Raposo, M. I. B., Ernesto, M., and Renne, P. R. (1998). Paleomagnetism and dating of the Early Cretaceous florianópolis dike swarm (santa catarina island), southern Brazil. *Phys. Earth Planet. Interiors* 108, 275–290. doi:10.1016/S0031-9201(98)00102-2

Renne, P. R., Deckart, K., Ernesto, M., Féraud, G., and Piccirillo, E. M. (1996). Age of the ponta grossa dike swarm (brazil), and implications to parana´flood volcanism. *Earth Planet. Sci. Lett.* 144, 199–211. doi:10.1016/0012-821x(96)00155-0

Reston, T. J. (2007). The formation of non-volcanic rifted margins by the progressive extension of the lithosphere: the example of the West Iberian margin. *Geol. Soc. Lond. Spec. Publ.* 282 (1), 77–110. doi:10.1144/SP282.5

Reston, T., and Manatschal, G. (2011). Rifted margins: building blocks of later collision. *Front. Earth Sci.*, 3–21. doi:10.1007/978-3540-88558-0_1

Reynolds, S. J. (1985). *Geology of the south Mountains, central Arizona. Arizona bureau of geology and mineral technology*, 195. Geological Survey Bulletin.

Rigoti, C. A. (2015). *Evolução tectônica da Bacia de Santos com ênfase na geometria crustal: interpretação integrada de dados de sísmica de reflexão e refração. Master thesis*. Universidade do Estado do Rio de Janeiro.

Ros, E., Pérez-Gussinyé, M., Araújo, M., Thoaldo Romeiro, M., Andrés-Martínez, M., and Morgan, J. P. (2017). Lower crustal strength controls on melting and serpentinization at magma-poor margins: potential implications for the south Atlantic. *Geochem. Geophys. Geosystems* 18 (12), 4538–4557. doi:10.1002/2017gc007212

Santos Neto, E. V., Cerqueira, J. R., and Prinzhofer, A. (2012). *Origin of CO2 in Brazilian basins*. Search and Discovery. Article #40969.

Sapin, F., Ringenbach, J. C., and Clerc, C. (2021). Rifted margins classification and forcing parameters. *Sci. Rep.* 11, 8199. doi:10.1038/s41598-021-87648-3

Schmitt, R. S., Trouw, R. A. J., Medeiros, S. R., and Dantas, E. L. (2008). Age and geotectonic setting of late Neoproterozoic juvenile mafic gneisses and associated paragneisses from the ribeira belt (SE Brazil) based on geochemistry and Sm–Nd data — implications on gondwana assembly. *Gondwana Res.* 13, 502–515. doi:10.1016/j.gr.2007.05.015

Schmitt, R. S., Trouw, R. A. J., Schmus, W. R., Armstrong, R., and Stanton, N. S. G. (2016). The tectonic significance of the cabo frio tectonic domain in the SE Brazilian margin: a Paleoproterozoic through Cretaceous Saga of a reworked Continental margin. *Braz. J. 302 Genet.* 46, 37–66. doi:10.1590/2317-4889201620150025

Schmitt, R. D. S., Fragoso, R. D. A., and Collins, A. S. (2018). Suturing gondwana in the Cambrian: the orogenic events of the final amalgamation. *Geol. southwest Gondwana*, 411–432. doi:10.1007/978-3-319-68920-3_15

Spadini, A. R., Esteves, F. R., Dias-Brito, D., Azevedo, R. L. M., and Rodrigues, R. (1988). The Maca´e formation, campos basin, Brazil: its evolution in the context of the initial history of the south Atlantic. *Rev. Bras. Geociencias* 18 (3), 261–272. doi:10.25249/0375-7536.1988261272

Stanton, N., Ponte-Neto, C., Masini, E., Bijani, R., Fontes, S., and Flexor, J.-M. (2014). A geophysical view of the southeastern Brazilian margin at santos basin: insights into rifting evolution. *J. S. Am. Earth Sci.* 55, 141–154. doi:10.1016/j.jsames.2014.07.003

Stanton, N., Kusznir, N., Gordon, A., and Schmitt, R. S. (2019). Architecture and Tectono magmatic evolution of the campos rifted margin: control of OCT structure by basement inheritance. *Mar. Petroleum Geol.* 100, 43–59. doi:10.1016/j.marpetgeo.2018.10.043

Stica, J. M., Zalán, P. V., and Ferrari, A. L. (2014). The evolution of rifting on the volcanic margin of the pelotas basin and the contextualization of the paraná–etendeka LIP in the separation of gondwana in the south Atlantic. *Mar. Petroleum Geol.* 50, 1–21. doi:10.1016/j.marpetgeo.2013.10.015

Strugale, M., Schmitt, R., and Cartwright, J. (2021). Basement geology and its controls on the nucleation and growth of rift faults in the northern Campos Basin, offshore Brazil. *Basin Res.* 33 (3), 1906–1933. doi:10.1111/bre.12540

Sutra, E., and Manatschal, G. (2012). How does the continental crust thin in a hyperextended rifted margin? Insights from the iberia margin. *Geology* 40 (2), 139–142. doi:10.1130/G32786.1

Szatmari, P., and Milani, E. J. (2016). Tectonic control of the oil-rich large igneous-carbonate-salt province of the south Atlantic rift. *Mar. Petroleum Geol.* 77, 567–596. doi:10.1016/j.marpetgeo.2016.06.004

Talwani, M. (1965). "Computation with help of a digital computer of magnetic anomalies caused by bodies of arbitrary shape,"*Geophysics*, 30. Tulsa, 797–817. doi:10.1190/1.1439654

Talwani, M., and Abreu, V. (2000). Inferences regarding initiation of Oceanic crust formation from the U.S. east Coast margin and conjugate south Atlantic margins. *Geophys. Monogr.* 115, 211–233. doi:10.1029/GM115p0211

Tommasi, A., and Vauchez, A. (2001). Continental rifting parallel to ancient collisional belts: an effect of the mechanical anisotropy of the lithospheric mantle. *Earth Planet Sci. Lett.* 185, 199–210. doi:10.1016/S0012-821X(00)00350-2

Vieira, T. A. T., Schmitt, R. S., Mendes, J. C., Moraes, R., Luvizotto, G. L., de Andrade Silva, R. L., et al. (2022). Contrasting p–t–t paths of basement and cover within the búzios orogen, SE Brazil: tracking Ediacaran–Cambrian subduction zones. *Precambrian Res.* 368, 106479. article 106479. doi:10.1016/j.precamres.2021.106479

Wernicke, B. (1985). Uniform-sense normal simple shear of the Continental lithosphere. *Can. J. Earth Sci.* 22, 108–125. doi:10.1139/e85-009

White, R., and Mckenzie, D. (1989). Magmatism at rift zones — the generation of volcanic Continental margins and flood basalts. *J. Geophys. Res. Solid* 94, 7685–7729. doi:10.1029/jb094ib06p07685

White, R. S., Smith, L. K., Roberts, A. W., Christie, P. F., Kusznir, N. J., Roberts, A. M., et al. (2008). Lower-crustal intrusion on the north Atlantic Continental margin. *Nature* 452, 460–464. doi:10.1038/nature06687

Whitmarsh, R. B., White, R. S., Horsefield, S. J., Sibuet, J. C., Recq, M., and Louvel, V. (1996). "The ocean-continent boundary off the Western Continental margin of iberia: crustal structure west of Galicia bank,"*J. Geophys. Res.*, 101. Washington, 28291–28314. doi:10.1029/96jb02579

Whitmarsh, R. B., Manatschal, G., and Minshull, T. A. (2001). Evolution of magma-poor Continental margins from rifting to seafloor spreading. *Nature* 413 (6852), 150–154. doi:10.1038/35093085

Whitney, D. L., Teyssier, C., Rey, P., and Buck, W. R. (2013). Continental and Oceanic core complexes. *Geol. Soc. Am. Bull.* 125, 273–298. doi:10.1130/b30754.1

Zalán, P. V., Severino, M. D. C. G., Rigoti, C. A., Magnavita, L. P., Oliveira, J. A. B., and Vianna, A. R. (2011). An entirely new 3D-view of the crustal and mantle structure of a south Atlantic passive margin–Santos, campos and Espírito Santo basins, Brazil. *AAPG Annu. Conf. Exhib.* 10, 13.

Zwaan, F., Schreurs, G., and Rosenau, M. (2020). Rift propagation in rotational *versus* orthogonal extension: insights from 4D analogue models. *J. Struct. Geol.* 135, 103946. doi:10.1016/j.jsg.2019.103946